

Supporting Information

Synthesis and Electron Spin Relaxation of Tetra-Carboxylate Pyrroline

Nitroxides

Shengdian Huang,^{†, #} Joseph T. Paletta,^{†, #} Hanan Elajaili,[§] Kirby Huber,[§] Maren Pink,[‡] Suchada

Rajca,[†] Gareth R. Eaton,[§] Sandra S. Eaton,^{,§} Andrzej Rajca^{*,†}*

Department of Chemistry, University of Nebraska, Lincoln, Nebraska 68588-0304

Department of Chemistry and Biochemistry, University of Denver, Denver, CO 80208-2436

IUMSC, Department of Chemistry, Indiana University, Bloomington, Indiana 47405-7102

E-mail address: arajca1@unl.edu

[†] University of Nebraska

[§] University of Denver

[‡] Indiana University

[#]SH and JTP contributed equally to this work.

Table of Contents

1. Complete Reference 36 (p. S3).
2. General Procedures and Materials (p. S3).
3. X-ray Crystallography (Tables S1–S3 and Figures S1–S3; pp. S3 – S10).
4. EPR Spectroscopy at DU (Figures S4 – S6; pp. S11 – S14).
5. CW EPR Spectroscopy at UNL (Figs. S7 – S9, pp. S15 – S17).
6. DFT Calculations at UNL (Tables S4 – S7, Figure S10; pp. S18 – S20).
7. Synthesis of Nitroxides (pp. S21 – S26).
8. Spectra of Nitroxides (Paramagnetic ^1H NMR and IR), and Spectra of Diamagnetic Synthetic Intermediates and Hydroxylamines (Figures S11 – S39; pp. S27–S41).
9. Supporting References (p. S42).
10. Cartesian Coordinates for UB3LYP/6-311+G(d,p)+ZPVE Geometries for the Lowest Energy Conformations of Nitroxides 1 and 2 (pp. S43–end).

1. Complete Reference 36.

36. Frisch, M. J.; Trucks, G. W.; Schlegel, H. B.; Scuseria, G. E.; Robb, M. A.; Cheeseman, J. R.; Scalmani, G.; Barone, V.; Mennucci, B.; Petersson, G. A.; Nakatsuji, H.; Caricato, M.; Li, X.; Hratchian, H. P.; Izmaylov, A. F.; Bloino, J.; Zheng, G.; Sonnenberg, J. L.; Hada, M.; Ehara, M.; Toyota, K.; Fukuda, R.; Hasegawa, J.; Ishida, M.; Nakajima, T.; Honda, Y.; Kitao, O.; Nakai, H.; Vreven, T.; Montgomery, Jr., J. A.; Peralta, J. E.; Ogliaro, F.; Bearpark, M.; Heyd, J. J.; Brothers, E.; Kudin, K. N.; Staroverov, V. N.; Kobayashi, R.; Normand, J.; Raghavachari, K.; Rendell, A.; Burant, J. C.; Iyengar, S. S.; Tomasi, J.; Cossi, M.; Rega, N.; Millam, N. J.; Klene, M.; Knox, J. E.; Cross, J. B.; Bakken, V.; Adamo, C.; Jaramillo, J.; Gomperts, R.; Stratmann, R. E.; Yazyev, O.; Austin, A. J.; Cammi, R.; Pomelli, C.; Ochterski, J. W.; Martin, R. L.; Morokuma, K.; Zakrzewski, V. G.; Voth, G. A.; Salvador, P.; Dannenberg, J. J.; Dapprich, S.; Daniels, A. D.; Farkas, Ö.; Foresman, J. B.; Ortiz, J. V.; Cioslowski, J.; Fox, D. J. *Gaussian 09*, Revision A.1 (Gaussian, Inc., Wallingford CT, 2009).

2. General Procedures and Materials.

Throughout the following paragraphs labels “JTP12-97f1C” and alike correspond to sample or experiment codes directly traceable to the laboratory notebooks or raw data.

3. X-ray Crystallography.

Data collection, structure solution, and refinement are briefly summarized below; more detailed descriptions may be found in the accompanying crystallographic information files (CIFs).

For nitroxides **1** and **2**, the structures were determined using crystals obtained by slow evaporation of a DCM/heptane (1:1) solution (label: JTP12-97f1C) and vapor diffusion of pentane into a chloroform solution (label: HSD-1-1-26), respectively.

Nitroxide 1. A colorless crystal (approximate dimensions $0.25 \times 0.18 \times 0.10 \text{ mm}^3$) was placed onto the tip of a 0.05 mm diameter glass capillary and mounted on a commercial diffractometer equipped with a detector at 150(2) K. The data collection was carried out using Mo K α radiation (graphite monochromator) with a frame time of 30 seconds and a detector distance of 40 mm. The total exposure time was 18.12 hours. The frames were integrated with the SAINT software package^{S1} using

a narrow-frame algorithm. The integration of the data using a monoclinic unit cell yielded a total of 23212 reflections to a maximum θ angle of 26.45° (0.80 \AA resolution), of which 2949 were independent (average redundancy 7.871, completeness = 99.6%, $R_{\text{int}} = 3.33\%$, $R_{\text{sig}} = 1.90\%$) and 2524 (85.59%) were greater than $2\sigma(F_2)$. The final cell constants of $a = 16.1787(15) \text{ \AA}$, $b = 7.8957(7) \text{ \AA}$, $c = 11.6365(10) \text{ \AA}$, $\beta = 105.489(5)^\circ$, volume = $1432.5(2) \text{ \AA}^3$, are based upon the refinement of the XYZ-centroids of 9945 reflections above $20 \sigma(I)$ with $5.225^\circ < 2\theta < 52.71^\circ$. Data were corrected for absorption effects using the multi-scan method (SADABS).^{S2} The ratio of minimum to maximum apparent transmission was 0.890. The calculated minimum and maximum transmission coefficients (based on crystal size) are 0.9690 and 0.9870. Please refer to Table S1 for additional crystal and refinement information.

The space group $P2_1/c$ was determined based on intensity statistics and systematic absences. The structure was solved and refined using the SHELX suite of programs.^{S3} An intrinsic-methods solution was calculated, which provided most non-hydrogen atoms from the E-map. Full-matrix least squares / difference Fourier cycles were performed, which located the remaining non-hydrogen atoms. All non-hydrogen atoms were refined with anisotropic displacement parameters. The hydrogen atoms were placed in ideal positions and refined as riding atoms with relative isotropic displacement parameters. The final anisotropic full-matrix least-squares refinement on F_2 with 203 variables converged at $R_1 = 3.24\%$, for the observed data and $wR_2 = 8.65\%$ for all data. The goodness-of-fit was 1.028. The largest peak in the final difference electron density synthesis was $0.326 \text{ e}^-/\text{\AA}^3$ and the largest hole was $-0.204 \text{ e}^-/\text{\AA}^3$ with an RMS deviation of $0.040 \text{ e}^-/\text{\AA}^3$. On the basis of the final model, the calculated density was 1.466 g/cm^3 and $F(000)$, 660 e^- . The remaining electron density is minuscule and located on bonds.

Nitroxide 2 was studied with synchrotron radiation at the ChemMatCARS 15IDB beamline^{S4} at the Advanced Photon Source at Argonne National Lab, Chicago, utilizing the SCrAPS program.^{S5}

A yellow crystal (approximate dimensions $0.115 \times 0.061 \times 0.055 \text{ mm}^3$) was placed onto the tip of an ultra-thin glass rod and mounted on a D8 platform goniometer and measured at $100(2) \text{ K}$. The data collection was carried out using synchrotron radiation ($\lambda=0.41328 \text{ \AA}$, $E=30 \text{ keV}$, silicon 111 and 113 monochromators, two mirrors to exclude higher harmonics) with a frame time 0.3 seconds and a detector distance of 60 mm. The total exposure time was 0.09 hours. The frames were integrated with

the SAINT software package^{S1} using a narrow-frame algorithm. The integration of the data using a monoclinic unit cell yielded a total of 13679 reflections to a maximum θ angle of 16.92° (0.71 Å resolution), of which 2333 were independent (average redundancy 5.863, completeness = 97.9%, $R_{\text{int}} = 6.05\%$, $R_{\text{sig}} = 4.49\%$) and 1988 (85.21%) were greater than $2\sigma(F_2)$. The final cell constants of $a = 16.3051(7)$ Å, $b = 6.5192(3)$ Å, $c = 15.4278(6)$ Å, $\beta = 97.9090(10)^\circ$, volume = 1624.32(12) Å³, are based upon the refinement of the XYZ-centroids of 5581 reflections above $20 \sigma(I)$ with $4.869^\circ < 2\theta < 33.70^\circ$. Data were corrected for absorption effects using the multi-scan method (SADABS).^{S2} The ratio of minimum to maximum apparent transmission was 0.841. The calculated minimum and maximum transmission coefficients (based on crystal size) are 0.6260 and 0.7441. Please refer to Table S2 for additional crystal and refinement information.

The space group C2/c was determined based on intensity statistics and systematic absences. The structure was solved using and refined using the SHELX suite of programs.^{S3} An intrinsic methods solution was calculated, which provided most non-hydrogen atoms from the E-map. Full-matrix least squares / difference Fourier cycles were performed, which located the remaining non-hydrogen atoms. All non-hydrogen atoms were refined with anisotropic displacement parameters. The hydrogen atoms were placed in ideal positions and refined as riding atoms with relative isotropic displacement parameters. The final anisotropic full-matrix least-squares refinement on F₂ with 113 variables converged at $R_1 = 4.94\%$, for the observed data and $wR_2 = 15.13\%$ for all data. The goodness-of-fit was 1.230. The largest peak in the final difference electron density synthesis was 0.531 e⁻/Å³ and the largest hole was -0.699 e⁻/Å³ with an RMS deviation of 0.225 e⁻/Å³. On the basis of the final model, the calculated density was 1.408 g/cm³ and F(000), 724 e⁻. Nonclassical hydrogen bonds were observed (Figure S3 and Table S3).

Table S1. Crystal data and structure refinement for nitroxide **1** (X-ray label: 15131, sample label: JTP12-97f1C)

Empirical formula	C ₁₂ H ₁₄ N O ₉	
Formula weight	316.24	
Crystal color, shape, size	colorless block, 0.25 × 0.18 × 0.10 mm ³	
Temperature	150(2) K	
Wavelength	0.71073 Å	
Crystal system, space group	Monoclinic, P2 ₁ /c	
Unit cell dimensions	a = 16.1787(15) Å	α = 90°.
	b = 7.8957(7) Å	β = 105.489(5)°.
	c = 11.6365(10) Å	γ = 90°.
Volume	1432.5(2) Å ³	
Z	4	
Density (calculated)	1.466 Mg/m ³	
Absorption coefficient	0.128 mm ⁻¹	
F(000)	660	

Data collection

Diffractometer	APEX II Kappa Duo, Bruker
Theta range for data collection	1.306 to 26.451°.
Index ranges	-20 ≤ h ≤ 20, -8 ≤ k ≤ 9, -14 ≤ l ≤ 14
Reflections collected	23212
Independent reflections	2949 [R(int) = 0.0333]
Observed Reflections	2524
Completeness to theta = 25.242°	100.0 %

Solution and Refinement

Absorption correction	Semi-empirical from equivalents
Max. and min. transmission	0.7454 and 0.6634
Solution	Intrinsic methods
Refinement method	Full-matrix least-squares on F ²
Weighting scheme	w = [σ ² F _o ² + AP ² + BP] ⁻¹ , with P = (F _o ² + 2 F _c ²)/3, A = 0.0412, B = 0.6339
Data / restraints / parameters	2949 / 0 / 203
Goodness-of-fit on F ²	1.028
Final R indices [I > 2σ(I)]	R1 = 0.0324, wR2 = 0.0819
R indices (all data)	R1 = 0.0395, wR2 = 0.0865
Largest diff. peak and hole	0.326 and -0.204 e.Å ⁻³

Goodness-of-fit = [Σ[w(F_o² - F_c²)²]/N_{observns} - N_{params}]^{1/2}, all data.

R1 = Σ(|F_o - |F_c||) / Σ |F_o|. wR2 = [Σ[w(F_o² - F_c²)²] / Σ [w(F_o²)²]^{1/2}.

Table S2. Crystal data and structure refinement for nitroxide **2** (X-ray labels: S16003 and CMC1051, sample label: HSD-1-1-26).

Empirical formula	C ₁₄ H ₁₈ N ₉ O ₉
Formula weight	344.29
Crystal color, shape, size	yellow block, 0.115 × 0.061 × 0.055 mm ³
Temperature	100(2) K
Wavelength	0.41328 Å (30 keV)
Crystal system, space group	Monoclinic, C2/c
Unit cell dimensions	a = 16.3051(7) Å α = 90°. b = 6.5192(3) Å β = 97.909(1)°. c = 15.4278(6) Å γ = 90°.
Volume	1624.32(12) Å ³
Z	4
Density (calculated)	1.408 Mg/m ³
Absorption coefficient	0.072 mm ⁻¹
F(000)	724

Data collection

Diffractometer	APS, ChemMatCARS, 15 IDB
Theta range for data collection	1.550 to 16.916°.
Index ranges	-20 ≤ h ≤ 22, -9 ≤ k ≤ 9, -18 ≤ l ≤ 21
Reflections collected	13679
Independent reflections	2333 [R(int) = 0.0605]
Observed Reflections	1988
Completeness to theta = 14.357°	97.8 %

Solution and Refinement

Absorption correction	Semi-empirical from equivalents
Max. and min. transmission	0.7441 and 0.6260
Solution	Intrinsic methods
Refinement method	Full-matrix least-squares on F ²
Weighting scheme	w = [σ ² F _o ² + AP ² + BP] ⁻¹ , with P = (F _o ² + 2 F _c ²)/3, A = 0.0827, B = 0.2655
Data / restraints / parameters	2333 / 0 / 113
Goodness-of-fit on F ²	1.230
Final R indices [I > 2σ(I)]	R1 = 0.0494, wR2 = 0.1273
R indices (all data)	R1 = 0.0645, wR2 = 0.1513
Extinction coefficient	0.35(3)
Largest diff. peak and hole	0.531 and -0.699 e.Å ⁻³

Goodness-of-fit = $[\sum [w(F_o^2 - F_c^2)^2] / (N_{\text{observns}} - N_{\text{params}})]^{1/2}$, all data.

$R1 = \sum (|F_o| - |F_c|) / \sum |F_o|$. $wR2 = [\sum [w(F_o^2 - F_c^2)^2] / \sum [w(F_o^2)^2]]^{1/2}$.

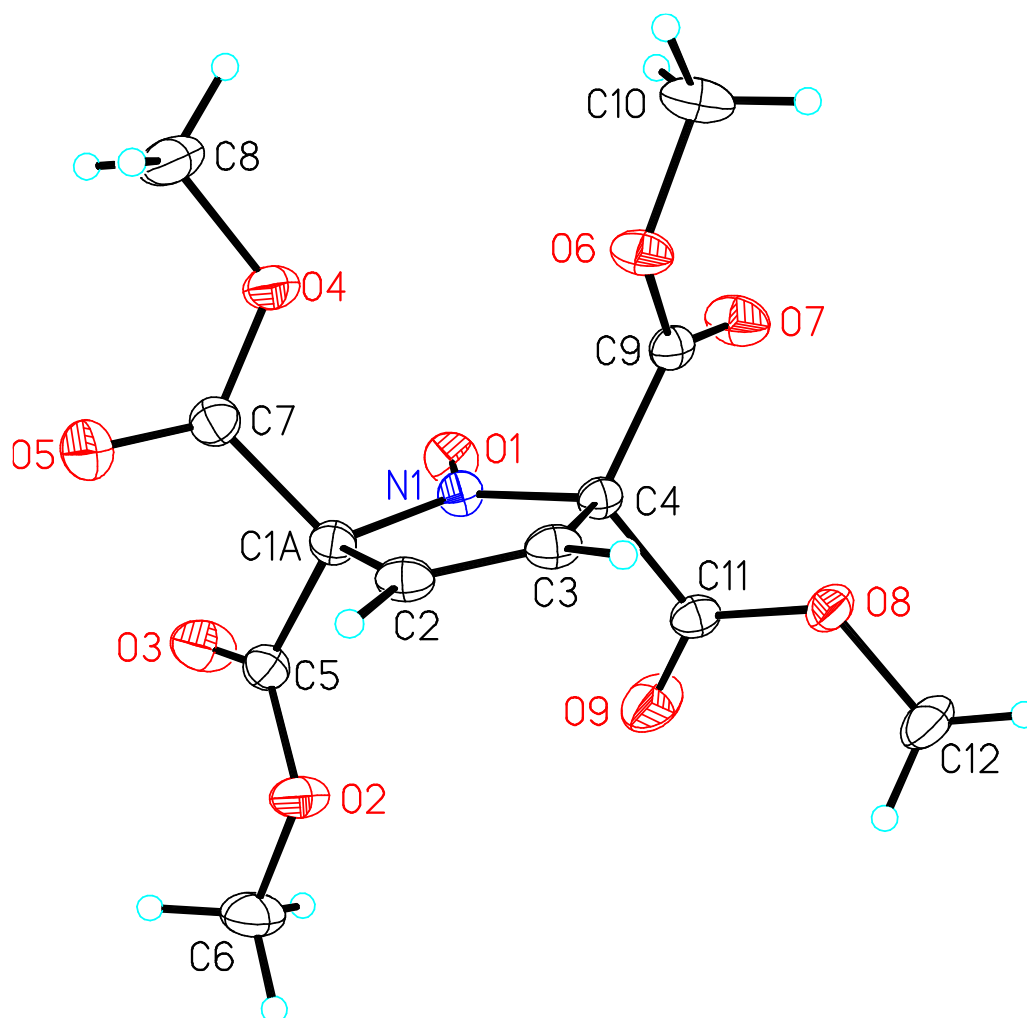
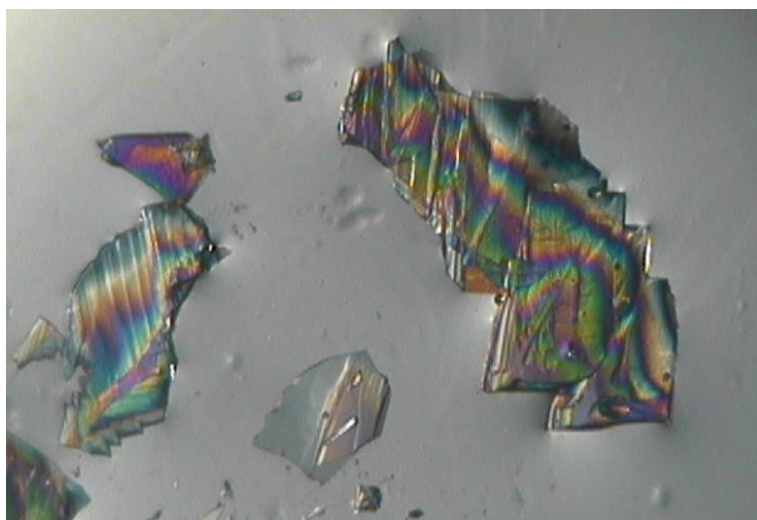


Figure S1. Nitroxide 1: formula unit obtained by Mo K α radiation (X-ray label: 15131, sample label: JTP12-97f1C). Carbon, nitrogen, and oxygen atoms are depicted with thermal ellipsoids set at the 50% probability level.

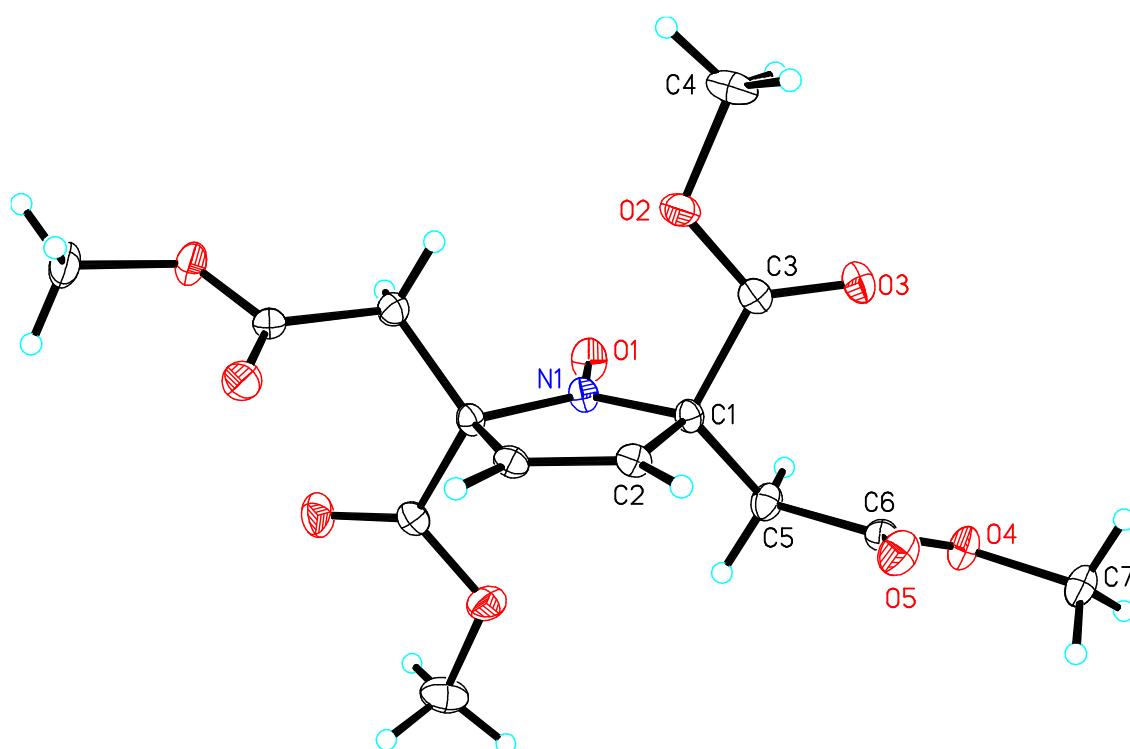
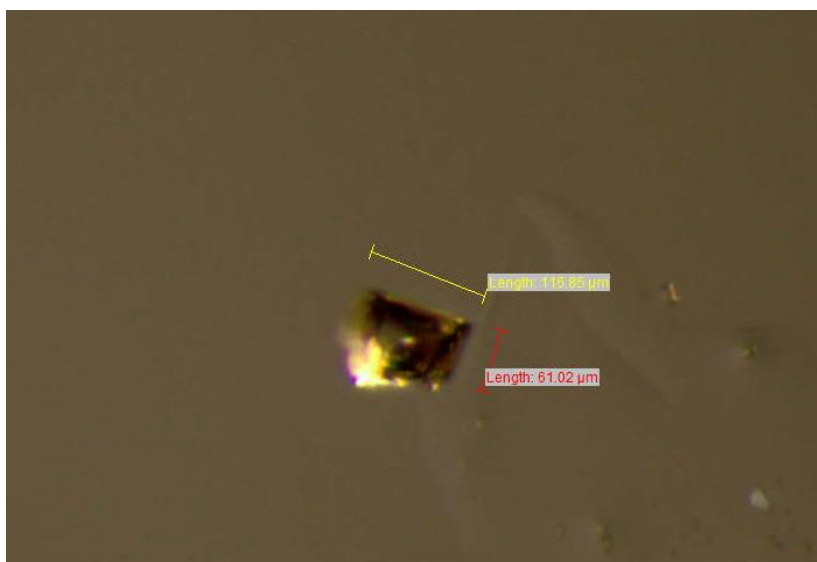


Figure S2. Nitroxide **2**: selected specimen and formula unit obtained by synchrotron radiation (X-ray labels: S16003 and CMC1051, sample label: HSD-1-1-26). Carbon, nitrogen, and oxygen atoms are depicted with thermal ellipsoids set at the 50% probability level.

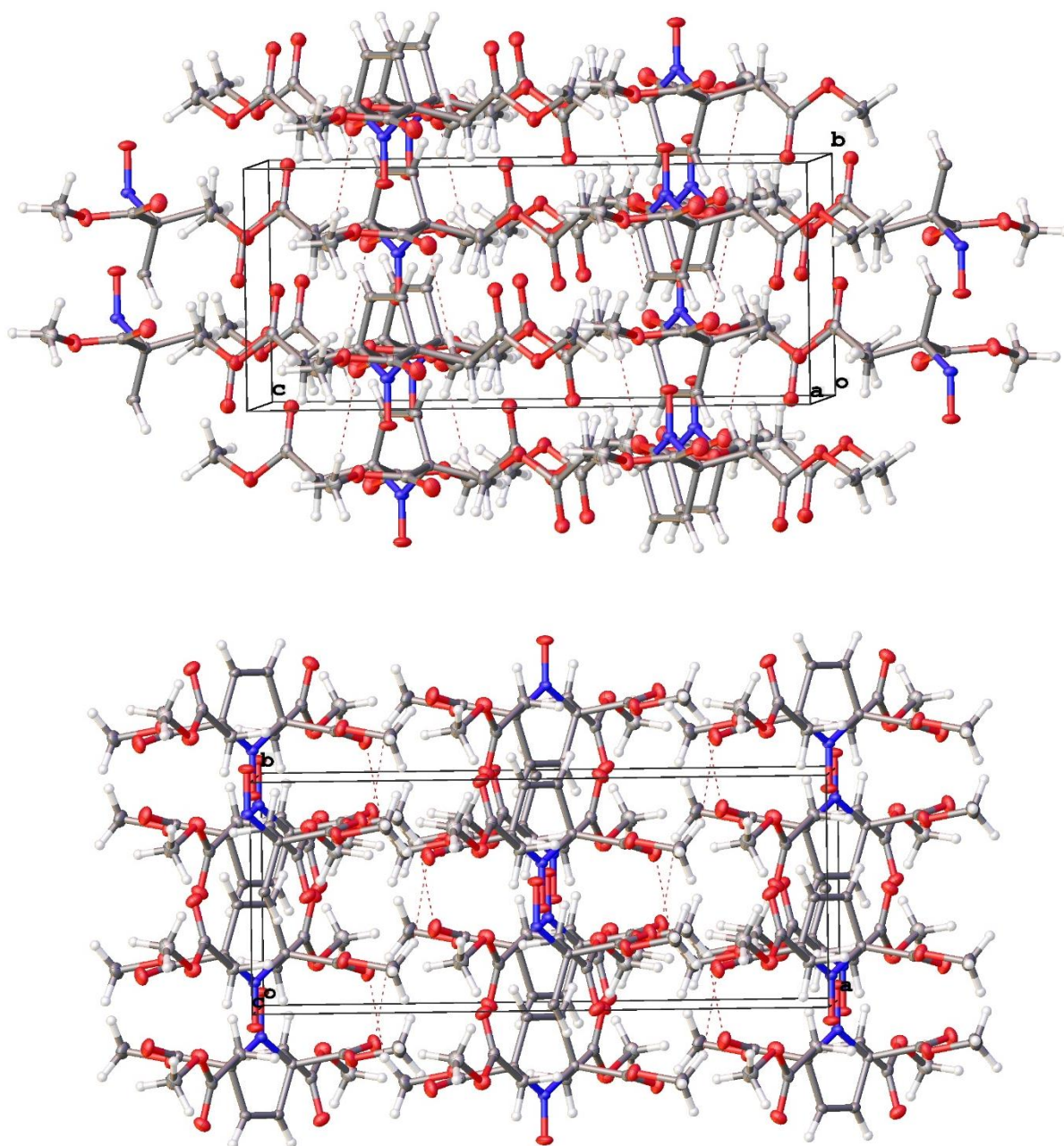


Figure S3. Nitroxide 2: cell plots, views along *a*-axis (top plot) and *c*-axis (bottom plot), showing nonclassical H-bonding (Table S3).

Table S3. Hydrogen bonds for nitroxide 2 (X-ray labels: S16003 and CMC1051) [\AA and $^\circ$].^a

D-H...A	d(D-H)	d(H...A)	d(D...A)	$\angle(\text{DHA})$
C2-H2...O1#2	0.95	2.56	3.1251(16)	118.5
C4-H4C...O3#3	0.98	2.53	3.4218(18)	151.8

^a Symmetry transformations used to generate equivalent atoms:

#1 $-x, y, -z+1/2$ #2 $x, y-1, z$ #3 $-x+1/2, y-1/2, -z+1/2$

4. EPR spectroscopy at DU.

X-band CW spectra were recorded on a commercial spectrometer with an SHQE resonator and 100 kHz modulation frequency. Variable temperature CW and pulse EPR experiments were obtained on a commercial spectrometer, which is equipped with an ER4118X-MS5 split ring resonator, a liquid helium cryostat, and a temperature controller for cryogenic temperatures. Q-band measurements were performed on a commercial instrument using an ER5107D2 resonator. Temperatures at the sample are accurate to within about 2 K. Spectra were simulated using the locally-written program Monmer, which is based on the equations in ref. S6. Parameters were adjusted to optimize agreement with spectra obtained at both X-band and Q-band. Relative g values were well defined in the Q-band spectra. The average g value was adjusted to agree with the values obtained for fluid solution spectra recorded with the dual mode resonator at the University of Nebraska (see below). A_z is well defined at both X-band and Q-band, but A_x and A_y are not resolved, so values of A_x and A_y were adjusted to make the average value agree with A_{iso} observed in fluid solution.

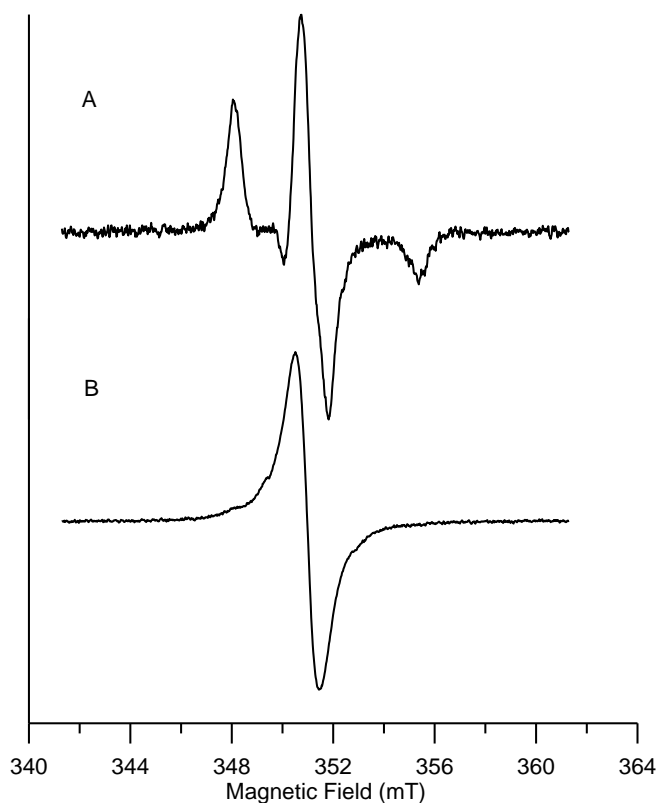


Figure S4. CW EPR (X-band, 9.862 GHz) spectra of tempol in trehalose at 20 °C.

A) magnetically dilute sample in well-formed glass obtained with 0.05 mT modulation amplitude at 100 kHz and 0.20 mW microwave power. B) Magnetically concentrated sample in a poorly-formed glass obtained with 0.1 mT modulation amplitude and 0.20 mW microwave power.

At room temperature the spectrum of tempol in a well-formed glassy matrix exhibits the anisotropic g and A -values that are characteristic of immobilized nitroxides (Figure S4A). However when there is not good glass formation and the solute is not magnetically dilute an exchange-narrowed spectrum is observed (Figure S4B). Samples may also be heterogenous resulting in spectra that are intermediate between those shown in Figure S4A and S4B. For small nitroxides such as tempol, it was difficult to reproducibly prepared well-formed glasses in trehalose. However, addition of 10% sucrose to the trehalose resulted in consistently well-formed glasses with magnetically dilute solute.

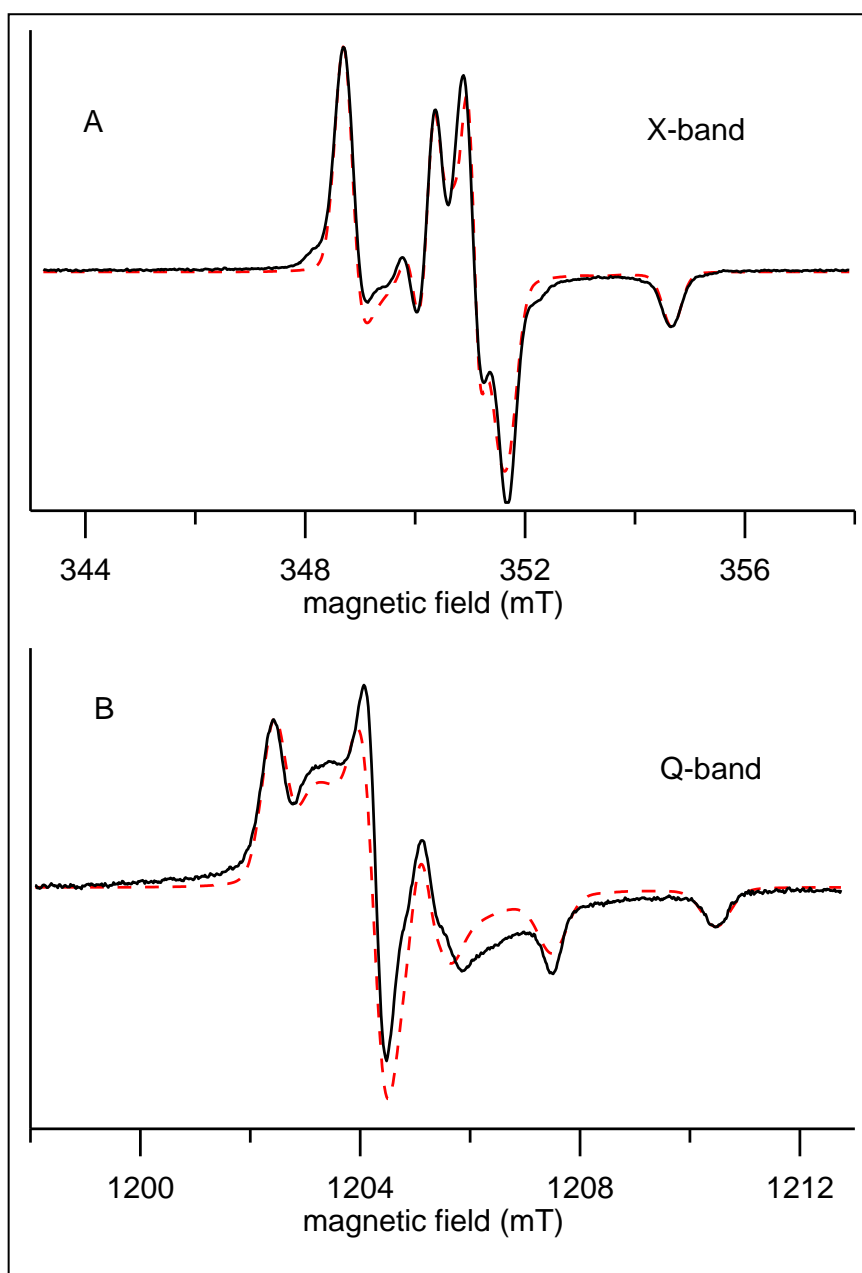


Figure S5. CW spectra of **1** in 9:1 trehalose:sucrose at 20°C (solid lines). A) X-band (9.857 GHz) spectrum obtained with 0.201 mW power and 0.1 mT modulation amplitude, and B) Q-band (33.84 GHz) spectrum obtained with 0.061 mW power and 0.1 mT modulation amplitude. The simulations (dashed red lines) were obtained with $g_x = 2.0099$, $g_y = 2.0060$, $g_z = 2.0025$, $A_x = 9.6$ MHz, $A_y = 9.8$ MHz, $A_z = 83.2$ MHz.

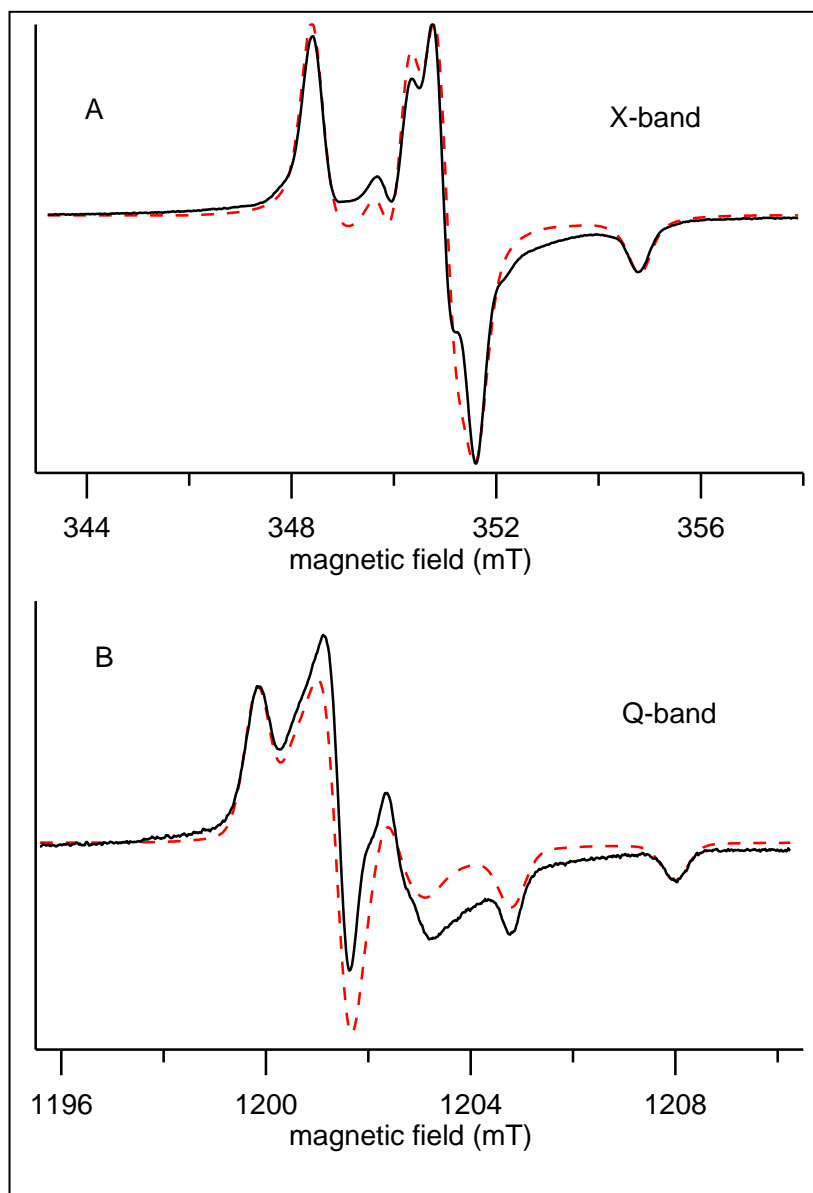


Figure S6. CW spectra of **2** in 9:1 trehalose:sucrose at 20 °C (solid lines). A) X-band (9.857 GHz) spectrum obtained with 0.201 mW power and 0.1 mT modulation amplitude, and B) Q-band (33.77 GHz) spectrum obtained with 0.061 mW power and 0.1 mT modulation amplitude. The simulations (dashed red lines) were obtained with $g_x = 2.0099$, $g_y = 2.0061$, $g_z = 2.0026$, $A_x = 12.0$ MHz, $A_y = 12.0$ MHz, $A_z = 89.0$ MHz

The broad underlying feature that is evident in the Q-band spectra of both **1** and **2**, but not in the simulated spectra suggests the presence of a small amount of magnetically-concentrated radical. The relaxation times of the magnetically concentrated radicals are much shorter than for the magnetically dilute material, and do not contribute to the measured relaxation times reported in the main text.

5. CW EPR spectroscopy at UNL.

CW X-band EPR spectra for nitroxides in solution were acquired on a commercial EPR instrument, equipped with a frequency counter and nitrogen flow temperature control (130–300 K). The spectra were obtained using a dual mode cavity; all spectra were recorded using an oscillating magnetic field perpendicular (TE_{102}) to the swept magnetic field. DPPH powder ($g = 2.0037$) was used as a g -value reference. The spectra were simulated using Symphonia or EasySpin (Garlic).

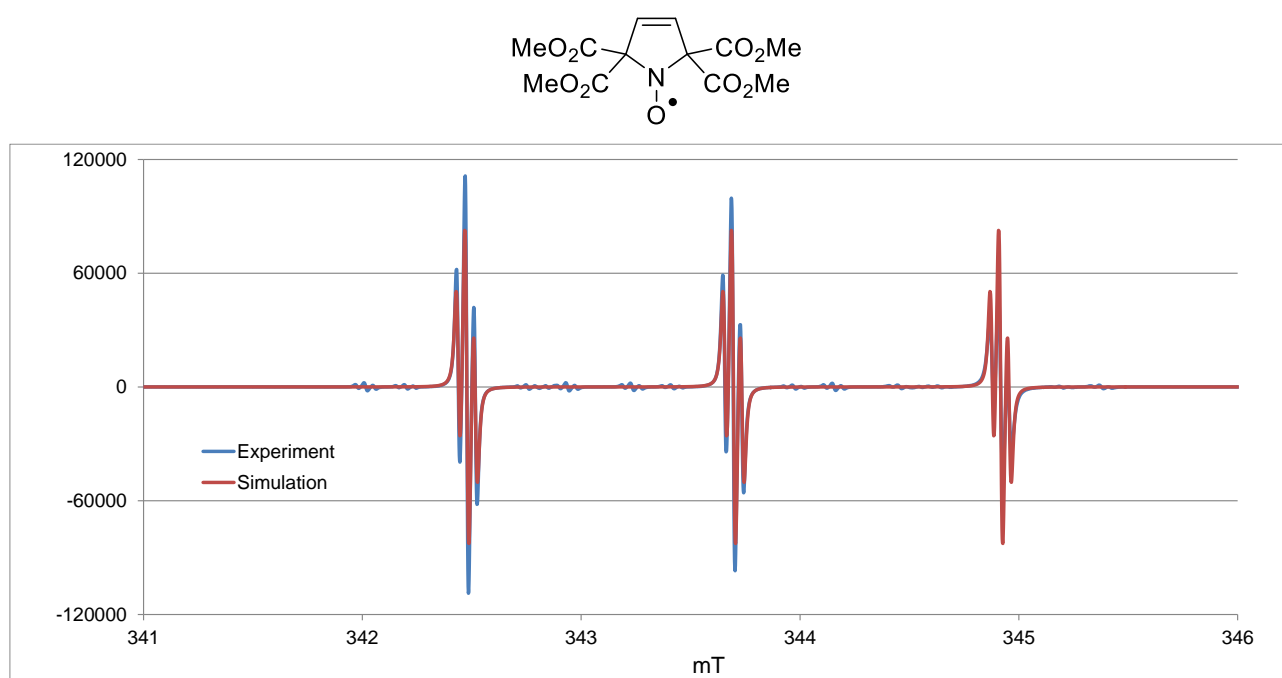


Figure S7. EPR ($\nu = 9.6505$ GHz) spectrum of nitroxide **1** (sample label: JTP13-21f1; 0.1 mM in CHCl_3 ; EPR label: HD174r1). Experimental spectrum: power, 20 dB, 2.046 mW; modulation amplitude 0.1 G; conversion time 40.96 ms; time constant 10.24 ms; resolution in X, 4k points. Simulation (EasySpin, Garlic): $g = 2.0061$, $A(^{14}\text{N}) = 34.223$ MHz ($n = 1$), $A(^1\text{H}) = 1.096$ MHz ($n = 2$), $\text{LW} = 0.0105$ mT (Gaussian) and 0.0132 mT (Lorentzian).

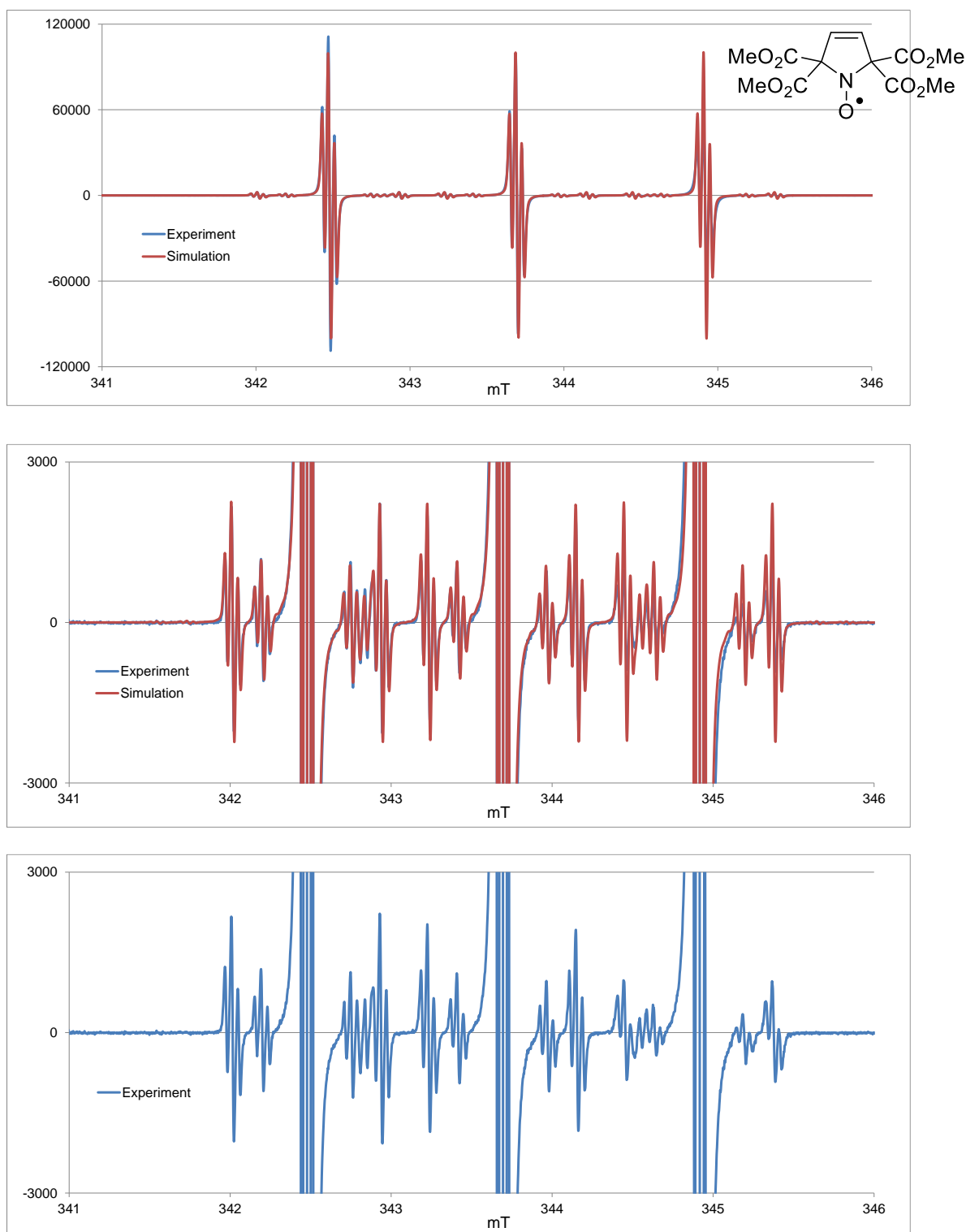


Figure S8. EPR ($\nu = 9.6505$ GHz) spectrum of nitroxide **1** (sample label: JTP13-21f1; 0.1 mM in CHCl_3 ; EPR label: HD174r1). Experimental spectrum: power, 20 dB, 2.046 mW; modulation amplitude 0.1 G; conversion time 40.96 ms; time constant 10.24 ms; resolution in X, 4k points. Simulation (Symphonia): $g = 2.0062$, $A(^{14}\text{N}) = 34.24$ MHz ($n = 1$), $A(^1\text{H}) = 1.096$ MHz ($n = 2$), $A(^{15}\text{N}) = 48.09$ MHz ($n = 1$), $A(^{13}\text{C}) = 25.30$ MHz ($n = 4$), $A(^{13}\text{C}) = 15.50$ MHz ($n = 2$), $L/G = 0.4$, $LW = 0.020$ mT. (All nuclei are at natural abundance.)

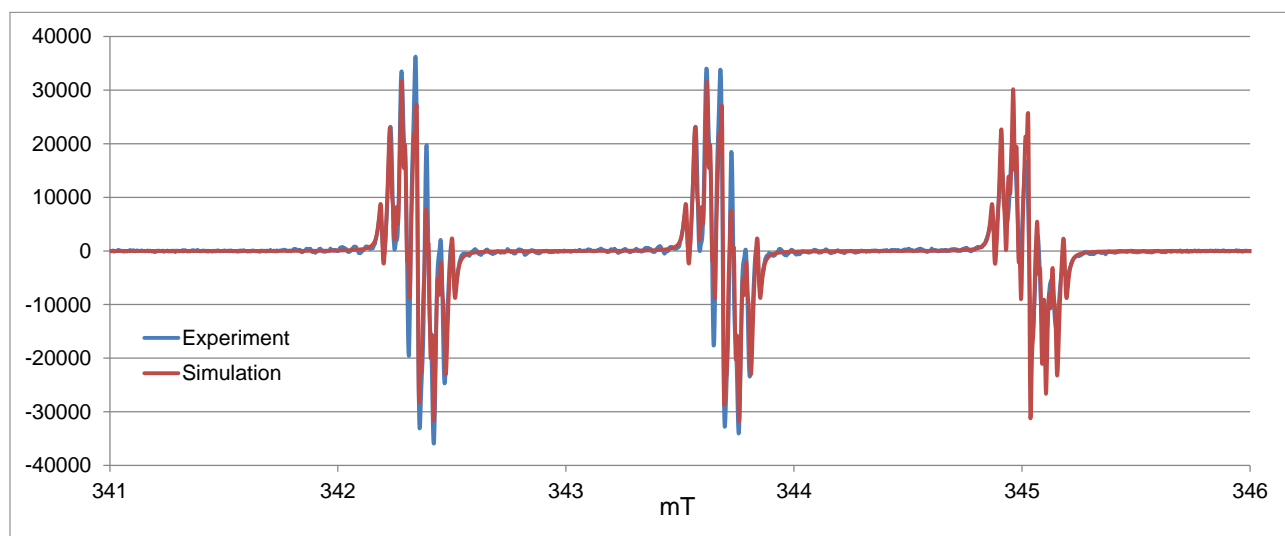
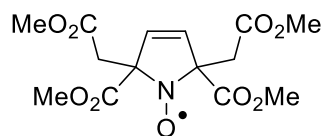


Figure S9. EPR ($\nu = 9.6499$ GHz) spectrum of nitroxide **2** (sample label: HSD1-1-26; 0.1 mM in CHCl_3 ; EPR label: HD174r2). Experimental spectrum: power, 20 dB, 2.046 mW; modulation amplitude 0.1 G; conversion time 40.96 ms; time constant 10.24 ms; resolution in X, 4k points. Simulation (EasySpin, Garlic): $g = 2.0060$, $A(^{14}\text{N}) = 37.648$ MHz ($n = 1$), $A(^1\text{H}) = 1.864$ MHz ($n = 2$), $A(^1\text{H}) = 1.430$ MHz ($n = 2$), $A(^1\text{H}) = 1.087$ MHz ($n = 2$), LW (Lorentzian) = 0.0147 mT.

6. DFT Calculations.

Geometry optimizations and frequency calculations were performed using the Gaussian 09 program package^{S7} running on a workstation under Linux operating system.

Ground-state geometries of nitroxides were optimized at the UB3LYP/6-311G(d,p) level. Starting geometry for **2** was the C_2 -symmetric conformation in the X-ray structure; this led to the lowest energy conformation for nitroxide **2**. The geometry optimizations were followed by vibrational analyses to confirm that all reported structures are the minima on the potential energy surface (Tables S4 and S5). These geometries were used for single point calculations of EPR spectral parameters at the UB3LYP/EPR-III level of theory (Table S6).

Stick and space-filling plots for the lowest energy conformations of **1** and **2** the UB3LYP/6-311G(d,p)+ZPVE level are presented in Figure S10.

Table S4. The B3LYP/6-311G(d,p)+ZPVE calculations for tetraester nitroxide **1**: energies (E° , hartree), zero point vibrational energies (ZPVE, hartree),^a lowest vibrational frequencies (cm^{-1}), RMS gradient norms (a.u.),^b dipole moments (μ , D), and relative energy (kcal mol^{-1}) of nitroxide.

	Point group	O14-C9-C1-N7 O15-C11-C4-N7 O13-C10-C1-N7 O16-C12-C4-N7	$\langle S^2 \rangle$	E°	ZPVE	$E^\circ + \text{ZPVE}$	Rel. energy	RMS gradient norm ($\times 10^{-6}$)	Lowest vibrational frequencies (cm^{-1})	μ (D)
Con7 Of7 Of11	C_2	170.91, 99.65 99.65, 170.91	0.7537	-1197.70468172	0.265110	-1197.439572	0.00	0.28	21.3, 27.8 29.9, 49.1	2.10
Of8	C_2	-8.78, 102.56 102.56, -8.78,	0.7537	-1197.70442342	0.264969	-1197.439454	0.07	0.58	16.1, 35.1 44.1, 54.6	1.33
Rot7 Of7 Of9	C_2	105.76, -4.23, -4.23, 105.76	0.7537	-1197.70306057	0.264837	- 1197.438224	0.85	1.19	18.9, 23.7 30.1, 55.0	6.28
IRC# 1 and #3	C_1	174.90, -96.06 96.31, -175.97	0.7538	-1197.70293553	0.265031	-1197.437905	1.05	1.65	19.8, 22.5, 25.8, 39.9	2.40
Of1- Xray	C_1	-165.33, -107.96 4.66, -106.47	0.7538	-1197.70251344	0.264994	-1197.437519	1.28	1.71	20.6, 23.8, 30.1, 44.3	4.25
Of10	C_2	-160.99, -112.21 -112.21, -160.99	0.7538	-1197.70171489	0.265169	-1197.436546	1.90	1.53	11.6, 22.7 30.2, 43.5	0.60
Of12 _Xra yC2	C_2	-168.69, -104.62 -104.62, -168.69	0.7538	-1197.70165525	0.265174	-1197.436482	1.94	1.11	20.0, 21.4, 26.3, 42.5	1.26
Of2	C_{2v}	12.56, -12.56, -12.56, 12.56	0.7534	-1197.69001163	0.264570	-1197.425442	8.87	0.57	<i>i51.5, i46.2,</i> 20.7, 26.8	7.77
Of3	C_{2v}	-131.83, 131.83 131.83, -131.83	0.7538	-1197.69150284	0.264332	-1197.427171	7.78	0.05	<i>i59.6, i54.5,</i> 21.2, 24.5	4.64
Of4	C_s	111.94, -111.94, 155.92, -155.92	0.7538	-1197.70184716	0.265008	-1197.436839	1.71	1.17	<i>i13.7, 25.0,</i> 35.6, 37.6	1.61
Of5	C_s	0.54, -0.54 93.62, -93.62	0.7538	-1197.70147001	0.264694	-1197.436776	1.75	1.52	23.5, 24.5, 40.3, 47.4	2.06
Of6	C_s	19.20, -161.64 -19.20, 161.64	0.7535	-1197.69274219	0.264729	-1197.428013	7.25	0.79	<i>i58.0, i39.1,</i> 20.1, 36.6	6.45

^a 1 Hartree = 627.51 kcal mol^{-1} . ^b In Cartesian coordinates.

Table S5. The UB3LYP/6-311G(d,p)+ZPVE calculations for nitroxide **2**: energies (E° , hartree), zero point vibrational energies (ZPVE, hartree),^a lowest vibrational frequencies (cm^{-1}), RMS gradient norms (a.u.),^b and dipole moments (D).

Structure	Point group	O14-C11-C4-N7 C30-C9-C1-N7 O31-C30-C9-C1 O13-C10-C1-N7 C29-C12-C4-N7 O32-C29-C12-C4	$\langle S^2 \rangle$	E°	ZPVE	$E^\circ + \text{ZPVE}$	Rel. energy (kcal mol ⁻¹)	RMS gradient norm ($\times 10^{-6}$)	Lowest vibrational frequencies (cm^{-1})	μ (D)
Rot8/Xray	C ₂	-118.39, -178.42, 23.74 -118.39, -178.42, 23.74	0.7541	-1276.37925199	0.322612	-1276.056640	0.00	1.25	17.3, 25.0, 32.7, 35.6	1.35
Rot9	C ₂	69.01, -178.54, 10.73 69.01, -178.54, 10.73	0.7541	-1276.37760243	0.322552	-1276.055051	1.00	2.27	14.6, 25.1, 32.2, 32.6	0.90
Rot11/12	C ₂	-122.65, 175.51, -155.06 -122.65, 175.51, -155.06	0.7541	-1276.37350109	0.322627	-1276.050874	3.62	1.29	27.5, 28.2, 28.6, 41.3	5.90
Rot10	C ₂	73.90, 174.14, -162.51 73.90, 174.14, -162.51	0.7542	-1276.37200636	0.322317	-1276.049690	4.36	3.24	<i>i</i> 15.7, 22.1, 26.7, 40.1	2.88
Rot4/6/7	C ₂	-179.11, 66.48, 47.52 -179.11, 66.48, 47.52	0.7538	-1276.37132281	0.322711	-1276.048612	5.03	1.48	14.0, 23.8, 33.7, 36.6	0.12
Rot2/5	C ₂	-172.13, 53.74, -127.64 -172.13, 53.74, -127.64	0.7539	-1276.37082435	0.322700	-1276.048124	5.34	0.27	9.3, 29.8, 35.7, 42.1	1.07
Rot1	C ₂	8.03, -66.40, -57.51 8.03, -66.40, -57.51	0.7537	-1276.37067335	0.322979	-1276.047694	5.61	1.89	26.1, 32.7, 41.5, 53.8	1.50
Start	C ₂	-155.07, -86.60, -46.43 -155.07, -86.60, -46.43	0.7538	-1276.36990687	0.322673	-1276.047234	5.90	2.93	20.6, 24.6, 38.2, 39.0	0.66
Rot3	C ₂	11.65, 61.85, -136.20 11.65, 61.85, -136.20	0.7538	-1276.36870924	0.322459	-1276.046250	6.52	0.64	28.9, 39.6, 43.6, 52.1	4.57

1 Hartree = 627.51 kcal mol⁻¹. ^b In Cartesian coordinates.

Table S6. Single point energies and ¹⁴N, ¹H, and ¹³C hyperfine couplings (MHz) for the lowest energy conformations of **1** and **2** at the UB3LYP/EPR-III//UB3LYP/6-311G(d,p) level of theory vs. experimental values.^a

	E° (UB3LYP/EPR-III)	$\langle S^2 \rangle$	$A(^{14}\text{N})$ (MHz)		$A(^1\text{H})$ (MHz)							
			N-O		vinylic CH			OCH ₃		CH ₂		
			DFT	EPR ^a	DFT	EPR	NMR	DFT	NMR	DFT	EPR	NMR
1	-1197.91835553	0.7544	21.60	34.24	-1.68	1.10	-1.08	x	+0.034	x	x	x
2	-1276.60180954	0.7548	25.03	37.65	-1.80	1.43	-1.26	x	+0.058 +0.017	-1.37 -1.94	1.09 1.86	-1.6 ^b

^a Experimental values were obtained in chloroform or chloroform-*d* at room temperature. For experimental and simulated EPR spectra of **1** and **2**, see: Figures S7 – S9; for paramagnetic ¹H NMR spectra of **1** and **2** see: Figures S15, S16, S24 and S25. In DFT computations, no conformational analysis of the methyl groups was carried out, thus computed values of $A(^1\text{H})$ for the methyl groups are not reported. For C₂-symmetric conformation of **1**, computed $A(^{13}\text{C})$ (in MHz) hyperfine coupling constants were as follows: -16.9 for C1 and C4 (quaternary carbons), +30.5 and +22.2 (avg. = +26.4) for C9-C13 (carbonyl carbons), 0.23 and -0.11 (avg. = +0.06) for C21, C25, C29 and C33 (methyl carbons), and -0.50 for C2 and C3 (vinylic carbons); for a simulation of EPR spectrum of **1**, including ¹⁵N and ¹³C nuclei at natural abundance, see: Figures S7 and S8.

^b In ¹H NMR spectrum of **2**, a very broad peak at $\delta = -40$ ppm was tentatively assigned to diastereotopic CH₂ protons (Figures S24 and S25).

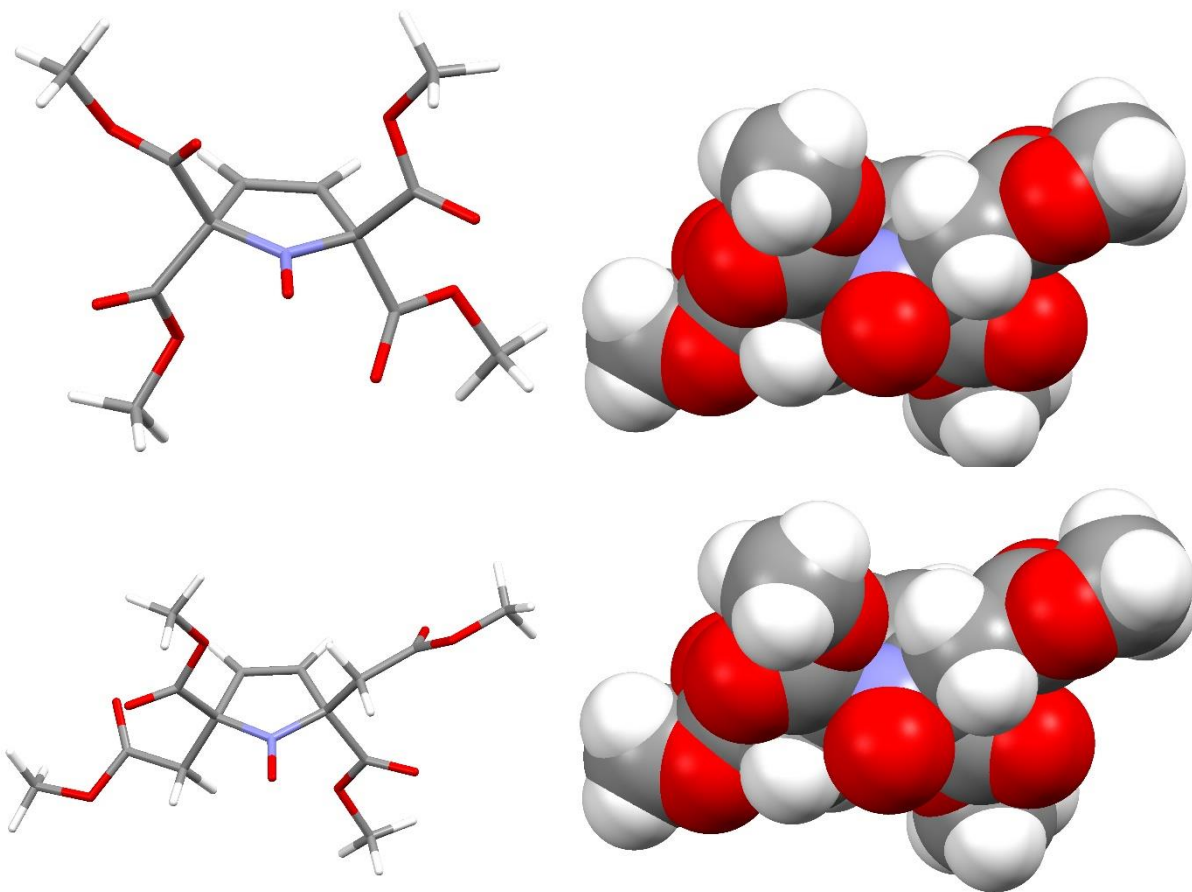
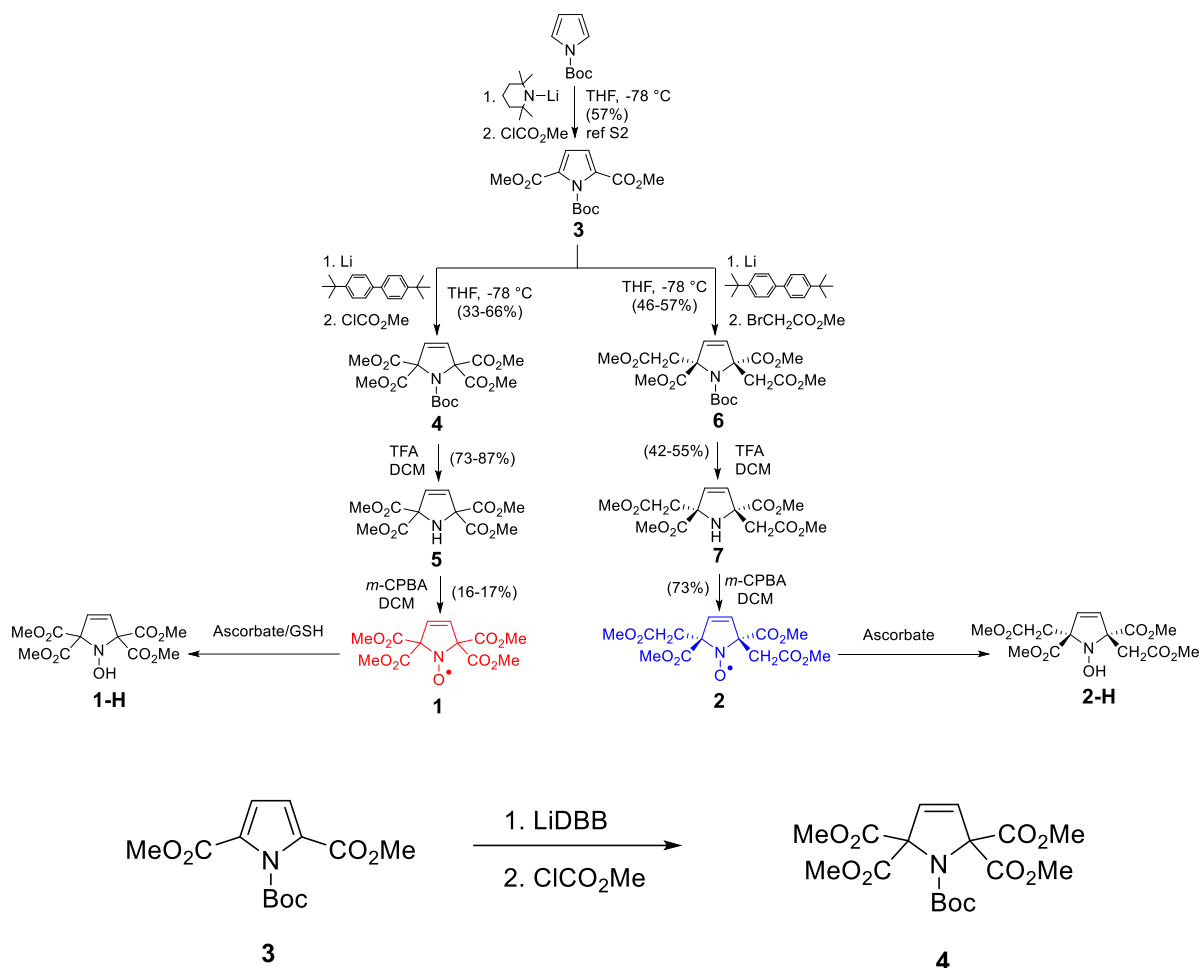


Figure S10. Stick and space-filling plots for the lowest energy conformations of nitroxides **1** (top) and **2** (bottom) computed at the UB3LYP/6-311G(d,p)+ZPVE level of theory.

7. Synthesis of Nitroxides.

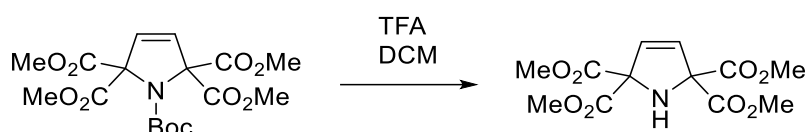
Synthetic scheme for preparation of nitroxides **1** and **2** is summarized below.



Label	SM Label	SM 3 (g/mmol)	THF (mL)	Li (g/mmol)	DBB (g/mmol)	ClCO ₂ Me (mL/mmol)	Yield (g/%)	Product label
JTP-9-31	JTP-9-27-fl	0.067/0.253	6.2	0.039/5.06	0.068/0.25	0.15/1.94	0.075/	JTP-9-31-fl
JTP-9-40	JTP-9-27-fl	1.089/3.84	49	0.440/63.4	0.512/1.92	1.2/15.5	0.515/33	JTP-9-40-fl
JTP-9-46	JTP-9-27-fl	5.633/19.9	240	2.23/321	2.631/9.88	6.2/80.2	4.667/58	JTP-9-46fl
JTP10-63	JTP10-56fl	4.190/14.78	220	1.95/281	1.872/7.03	4.6/59.53	1.167/20	JTP10-63fl
HSD-1-6	HSD-1-4	0.11/0.39	4.8	0.0435/6.22	0.0517/0.19	0.075/0.98	0.097/62	HSD-1-6
HSD-1-20	HSD-1-16	1.0/3.53	15	0.4/56.5	0.47/1.77	0.68/8.8	0.48/34	HSD-1-20
HSD-1-37	HSD-1-29	0.7/2.47	10.5	0.28/39.6	0.33/1.24	0.48/6.18	0.36/40	HSD-1-37
HSD-1-52	HSD-1-51	1.0/3.53	48	0.4/56.5	0.47/1.77	0.68/8.8	0.81/57	HSD-1-52
HSD-1-56	HSD-1-51	2.0/7.1	96	0.8/113	0.94/3.5	1.36/17.6	1.86/66	HSD-1-56

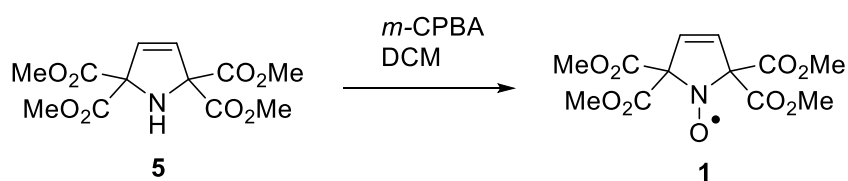
HSD-1-56: Lithium (0.80 g, 0.113 mol, surface was refreshed with razor) was washed with heptane, dried under vacuum, charged with argon, and cut into small pieces immediately before using. Tetrahydrofuran (16 mL, freshly distilled from sodium and benzophenone) was added to lithium and cooled to 0 °C. A solution of 4,4'-di-*tert*-butylbiphenyl (0.94 g, 3.5 mmol) in tetrahydrofuran (40 mL) was added to lithium dropwise; a blue color appeared immediately. After stirring for 3 h, the mixture was cooled to -78 °C and a solution of SM **3** (2.0 g, 7.1 mmol) in tetrahydrofuran (40 mL) was added dropwise; the reaction mixture became red shortly after the

addition, and then slowly became dark brown, to produce dianion of **3**.^{S8} After 16 h, the liquid was cannulated to mostly frozen methyl chloroformate (1.36 mL, 17.6 mmol) and stirred for 1 day at –78 °C. The reaction was quenched with saturated aqueous ammonium chloride (100 mL) and allowed to warm to rt. The mixture was diluted with ethyl ether (100 mL*3) and washed with brine (100 mL*3), dried over sodium sulfate and concentrated in rotatory evaporator. The crude was purified by column chromatography (silica gel, pentane/ethyl acetate, 1:1, R_f 0.32) to afford a light yellow solid (1.86 g, 66%).



Label	SM Label	SM 4 (g/mmol)	TFA (mL)	DCM (mL)	Yield (g/%)	Product label
JTP10-92	JTP10-63rc	0.157/0.391	10	25	0.086/73	JTP10-92ppt1
JTP12-1	JTP10-63rc	0.486/1.211	31	78	0.420	crude
JTP12-61	JTP12-7f2	2.637/6.570	145	350	1.720/87	JTP12-61f2

JTP12-61: SM **4** (2.64 g, 6.57 mmol) and dichloromethane (350 mL) were charged to a round bottom flask and cooled in an ice water bath. Trifluoroacetic acid (145 mL, 1.95 mol) was added dropwise and stirred for five minutes before removing the ice water bath. The solution was stirred for one hour until starting material could not be observed by thin layer chromatography, then the dichloromethane and trifluoroacetic acid were evaporated in a rotary evaporator. The resulting brown oil was dissolved in methanol (50 mL) and evaporated three times to yield the crude as a brown solid. The crude was washed over silica (silica gel, hexanes/ethyl acetate, 3:2) then eluted (methanol/dichloromethane, 3:97, R_f 0.48) to yield **5** as a sand colored solid (1.720 g, 87%).

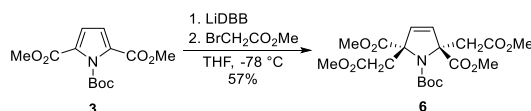


Label	SM Label	SM 5 (g/mmol)	DCM (mL)	<i>m</i> -CPBA (g/mmol)	Yield (g/%)	Product label	Spin conc. (%)
JTP12-90	JTP12-61f2	0.017/0.057	0.8	0.027/0.156	0.005/27	JTP12-90f1	75
JTP12-91	JTP12-61f2	0.006/0.020	0.7, Et ₂ O	0.008/0.046		Very low conversion	
JTP12-93	JTP12-61f2	0.022/0.073	0.8, Et ₂ O	0.031/0.180		Very low conversion	
JTP12-97	JTP12-61f2	0.194/0.644	7.5	0.405/2.346	0.039/19	JTP12-97f1	85
JTP12-98	JTP12-61f2	0.038/0.126	3, benzene	0.086/0.498	Crude	Broad nmr, not isolated	
JTP13-13	JTP12-61f2	0.849/2.817	33	1.826/10.58	0.145/16	JTP13-13f1	100
JTP13-21	JTP12-61f2	0.436/1.448	18	0.950/5.504	0.079/17	JTP13-21f1	99

JTP13-13: **5** (0.849 g, 2.82 mmol) was charged to a round bottom flask and evacuated for one hour then filled with nitrogen before being dissolved in dichloromethane (8.5 mL). The resulting solution was cooled in an ice water bath and purified *m*-CPBA^{S9} (1.83 g, 10.6 mmol) in dichloromethane (24 mL) was added dropwise. The resulting solution was stirred for five minutes, then the ice bath was removed. After three hours the solution was evaporated and dissolved in ethyl ether (70 mL), washed with saturated aqueous sodium bicarbonate until the aqueous layer was no longer yellow, washed with brine (2 × 15 mL), dried over sodium sulfate, and evaporated to give white powdery crude. The crude was purified with column chromatography (silica gel, chloroform/ethyl acetate, 2:1, R_f 0.45) to afford nitroxide **1** contaminated with *m*-CPBA as a slightly orange powder. The *m*-CPBA was removed by washing with ethyl ether (~20 × 1 mL) to afford **1** as an orange powder (145 mg, 16%). LRMS (ESI, 0.1% formic acid in methanol, label: JTP13-21f1): m/z ion type (%RA = percent relative amplitude for m/z 150–1000) 339 [M+Na]⁺ (60%), 655 [2M+Na]⁺ (100%), 671 [2M+K]⁺ (5%). A crystal suitable for X-ray crystallography was obtained by slow evaporation from a 1:1 DCM:heptane solution (label: JTP12-97f1C).

Reduction of nitroxide **1** to the corresponding hydroxylamine **1-H** using ascorbate.

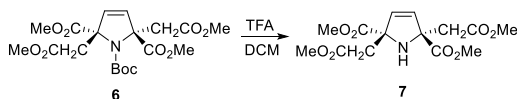
Nitroxide **1** (5.1 mg) was dissolved in ascorbate solution (2 mL, 20 mM ascorbate, 125 mM phosphate, 20 mM glutathione, pH 7.4) and allowed to react for 15 minutes. The solution was then saturated with sodium chloride, extracted with ethyl acetate (3 × 1 mL), dried over sodium sulfate, and evaporated yielding **1-H**. LRMS (ESI, 0.1% formic acid in methanol, label: JTP13-23-2): m/z ion type (%RA = percent relative amplitude for m/z 150–1000) 318 [M+H]⁺ (10%), 340 [M+Na]⁺ (30%), 657 [2M+Na]⁺ (100%).



Summary for preparation of compound **6**

Label	SM	SM	THF	Li	DBB	BrCH ₂ CO ₂ Me	Yield
	Label	(g/mmol)	(mL)	(g/mmol)	(g/mmol)	(mL/mmol)	(g/%)
HSD-1-1-10	HSD-1-1-4	0.11/0.389	2.4	0.04/6.224	0.052/0.2	0.143/1.56	0.077/46
HSD-1-1-12	HSD-1-1-5	1.0/3.532	24	0.4/56.5	0.47/1.77	1.30/14.13	0.71/47
HSD-1-1-24	HSD-1-1-5	0.45/1.590	12	0.18/25.44	0.212/0.8	0.59/6.36	0.38/57

6 (label: HSD-1-1-12): Lithium (0.4g, 56.5 mmol, surface was refreshed with razor) was washed with heptane, dried under vacuum, charged with argon, and cut into small pieces immediately before using. Tetrahydrofuran (4 mL, distilled from sodium and benzophenone) was added to lithium and cooled to 0 °C. A solution of 4,4'-di-*tert*-butylbiphenyl (0.47 g, 1.77 mmol) in tetrahydrofuran (10 mL) was added to lithium dropwise, a blue color appeared immediately. After stirring for 3 h, the mixture was cooled to -78 °C and a solution of SM **3** (1.0 g, 3.532 mmol) in tetrahydrofuran (10 mL) was added dropwise. Following the addition, the reaction mixture became red, and then slowly turn to dark brown.^{S8} After 16 h, the liquid was cannulated to mostly frozen methyl bromoacetate (1.30 mL, 14.13 mmol) and stirred for 1 day at -78 °C. The reaction was quenched with saturated aqueous ammonium chloride (30 mL) and allowed to warm to rt. The mixture was diluted with ethyl ether (30 mL*3) and washed with brine (30 mL*3), dried over sodium sulfate and concentrated in rotatory evaporator. The crude was purified by column chromatography (silica gel, pentane/ethyl acetate, 1:1, R_f 0.52) to afford a light yellow oil (710 mg, 47%). LRMS-ESI (0.1% HCOOH in MeOH, label: HSD-1-1-12), m/z (ion-type, % RA for m/z, 150-2000) at [M+Na]⁺: 452.2.

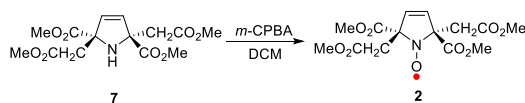


Summary for preparation of compound **7**

Label	SM Label	SM (g/mmol)	TFA (mL/mmol)	DCM (mL)	Yield (g/%)
HSD-1-1-14	HSD-1-1-12	0.4/0.932	2.4 /31.7	12	0.127/42
HSD-1-1-25	HSD-1-1-12, 24	0.6/1.40	3.6/47.6	18	0.25/54

7 (label: HSD-1-1-14): SM **6** (400 mg, 0.932 mmol) and dichloromethane (12 mL) were charged to a round bottom flask and cooled in an ice water bath. Trifluoroacetic acid (2.4 mL, 31.7 mmol) was added dropwise and stirred for five minutes before removing the ice water bath. The solution was stirred for two hours until starting material could not be observed by thin layer chromatography, then the dichloromethane and trifluoroacetic acid were evaporated in a rotary evaporator. The resulting brown oil was dissolved in methanol (5 mL) and evaporated (the dissolution and evaporation repeated three times), to yield the crude as a brown solid. The crude was purified by column chromatography (silica gel, pentane/ethyl acetate, 3:1, R_f 0.15) to afford a brown solid (127 mg, 42%). LRMS-ESI

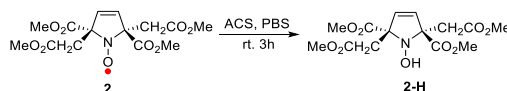
(0.1% HCOOH in MeOH, label: HSD-1-1-14), m/z (ion-type, % RA for m/z, 150-2000) at [M+Na]⁺: 352.2.



Summary for preparation of compound **2**

Label	SM Label	SM (g/mmol)	DCM (mL)	mCPBA (g/mmol)	Yield (g/%)	Spin conc. (%)
HSD-1-1-15	HSD-1-1-14	0.02/0.061	1.0	0.04/0.231	0.008/38	--
HSD-1-1-17	HSD-1-1-14	0.098/0.3	4.9	0.196/1.135	0.0353/35	~100
HSD-1-1-26	HSD-1-1-25	0.25/0.76	12.5	0.498/2.89	0.19/73	91

2 (label: HSD-1-1-26): SM **7** (250 mg, 0.76 mmol) was charged to a round bottom flask and evacuated for one hour then filled with nitrogen before being dissolved in dichloromethane (5.0 mL). The resulting solution was cooled in an ice water bath and purified *m*-CPBA^{S9} (498 mg, 2.89 mmol) in dichloromethane (7.5 mL) was added dropwise. The resulting solution was stirred for 5 min, then the ice bath was removed. After 2 h, the solvents were evaporated and the residue was dissolved in ethyl ether (15 mL), washed with saturated aqueous sodium bicarbonate until the aqueous layer was no longer yellow, washed with brine (3 × 15 mL), dried over sodium sulfate, and evaporated to give pale yellow powdery crude. The crude was purified with column chromatography (silica gel, pentane/ethyl acetate, 3:1, R_f 0.31) to afford a light yellow solid (190 mg, 73%). LRMS-ESI (0.1% HCOOH in MeOH, label: HSD-1-1-26), m/z (ion-type, % RA for m/z, 150-2000) at [M+Na]⁺: 367.6. Single crystal growth for X-ray crystallography: 20 mg of nitroxide **2** was dissolved in 1 ml of chloroform, and then was filtered to a small vial. This small vial was placed into a big vial containing 2 ml of pentane, and then after sealing the big vial, the assembly was left at room temperature for overnight. The crystal formation was observed next day.



Summary for preparation of compound **2-H**

2-H (label: HSD-1-1-36): Nitroxide **2** (label: HSD-1-1-26, 10.6 mg, 0.031 mmol, 1.0 equiv.) was dissolved into 2.5 ml of phosphate buffered saline (PBS; 12.4 mM) to give a homogenous solution. To this solution, L-ascorbic acid (ACS; 27.13 mg, 0.154 mmol, 5.0 equiv.) was added. The mixture

was stirred at ambient temperature with the protection from light for 3 hours. After 3 hours, the solutions was extracted with ethyl acetate (3 mL*3), and the organic layer was dried over Na₂SO₄ and concentrated under the reduced pressure, and then evacuated under high vacuum to afford the residue of the reaction of 7 mg (label: HSD-1-1-36). The residue was dissolved in CDCl₃ and characterized by NMR, IR and MS. LRMS-ESI (0.1% HCOOH in MeOH, HSD-1-1-36), m/z (ion-type, % RA for m/z, 150-2000) at [M+Na]⁺: 368.1.

8. Spectra of Nitroxides (Paramagnetic ^1H NMR and IR), and Spectra of Diamagnetic Synthetic Intermediates and Hydroxylamines.

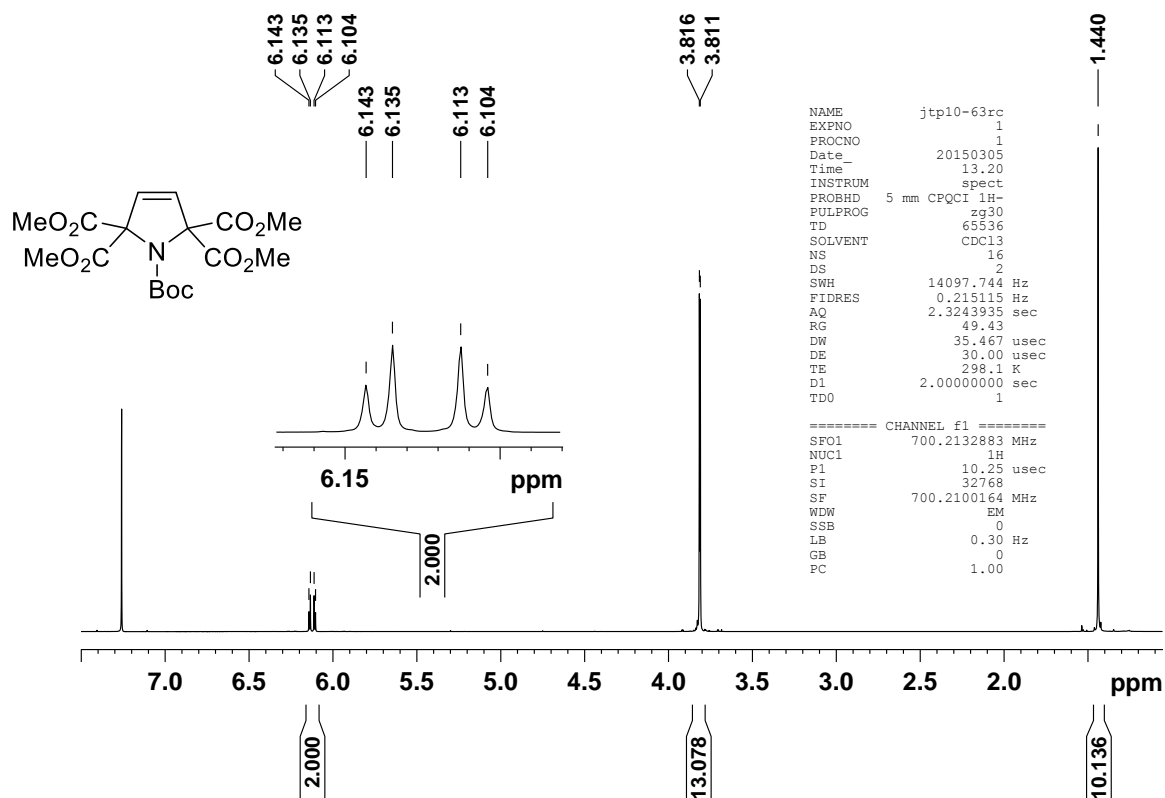


Figure S11. ^1H NMR spectrum (700 MHz, CDCl_3) of 4 (label: JTP10-63rc).

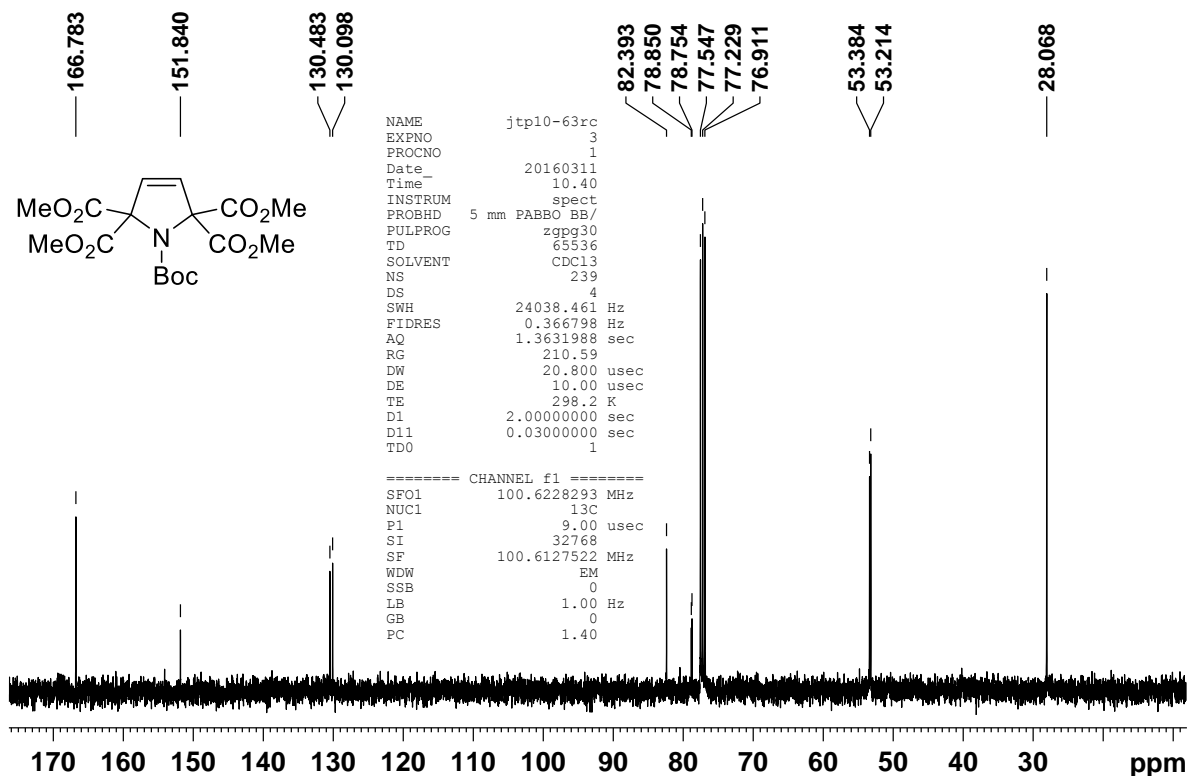


Figure S12. ^{13}C NMR spectrum (100 MHz, CDCl_3) of 4 (label: JTP10-63rc).

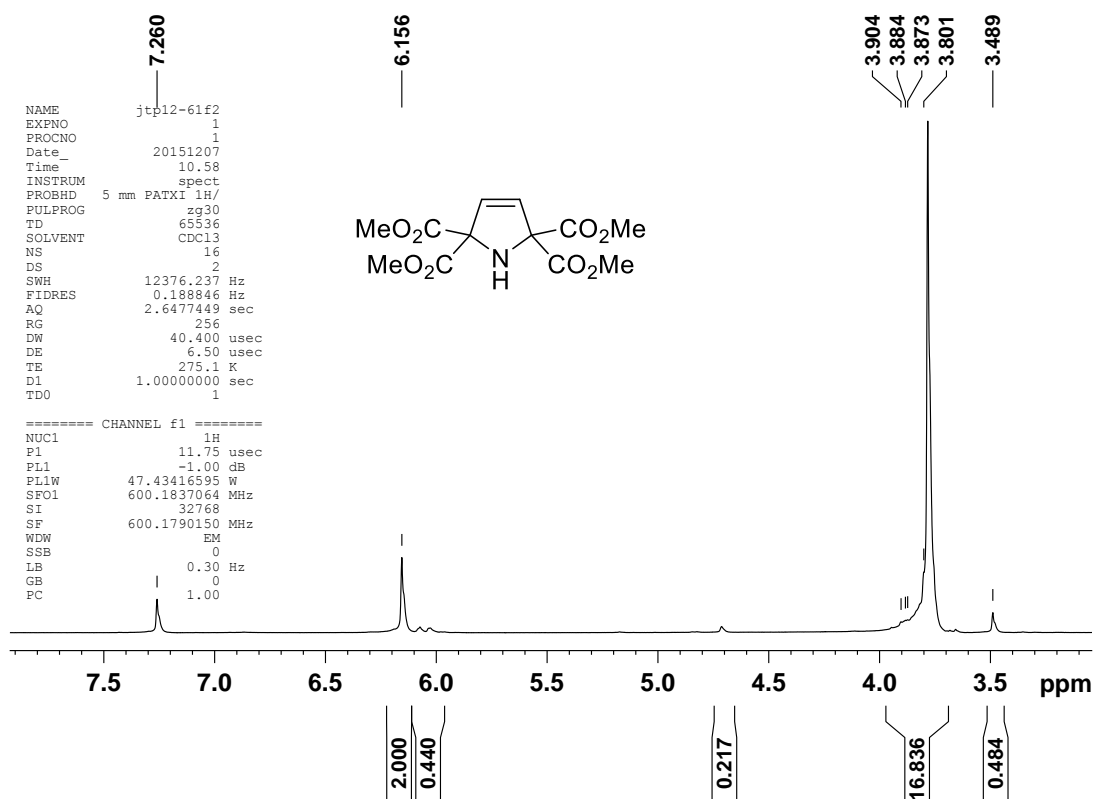


Figure S13. ¹H NMR spectrum (600 MHz, CDCl₃) of **5** (label: JTP12-61f2).

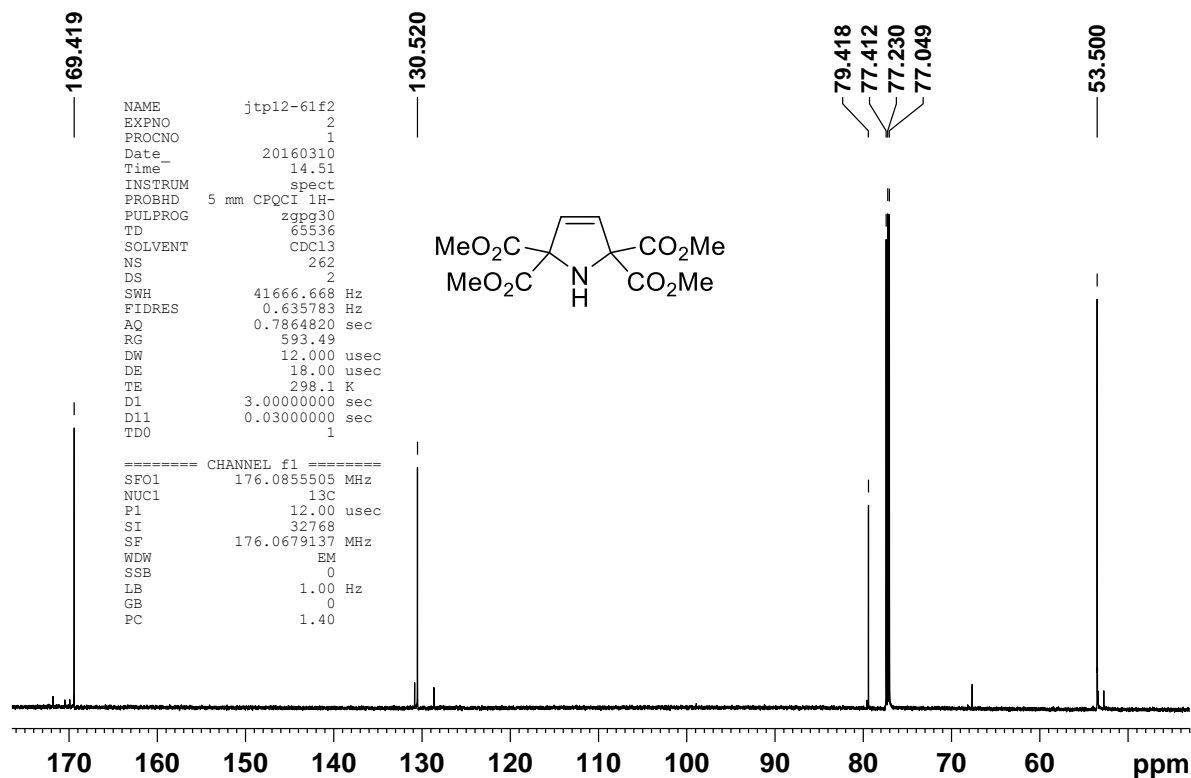


Figure S14. ¹³C NMR spectrum (176 MHz, CDCl₃) of **5** (label: JTP12-61f2).

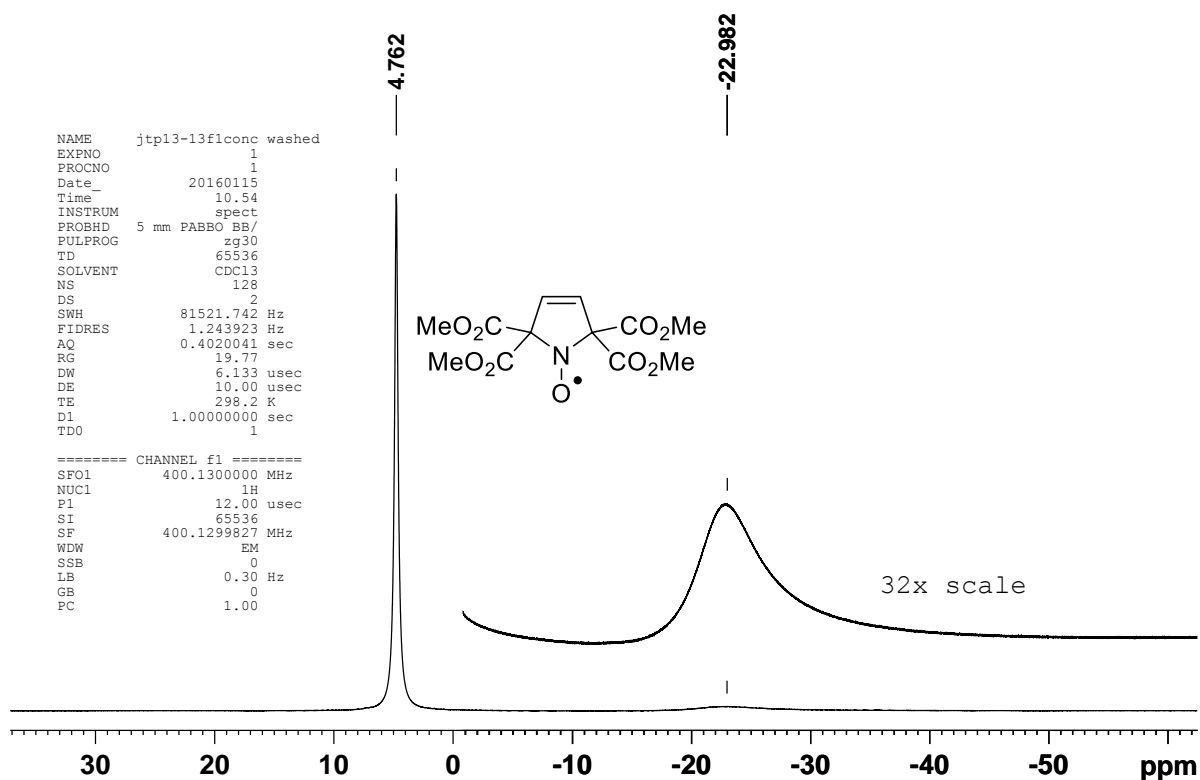


Figure S15. ¹H NMR spectrum (400 MHz, 0.9 M in CDCl₃) of nitroxide 1 (label: JTP13-31f1).

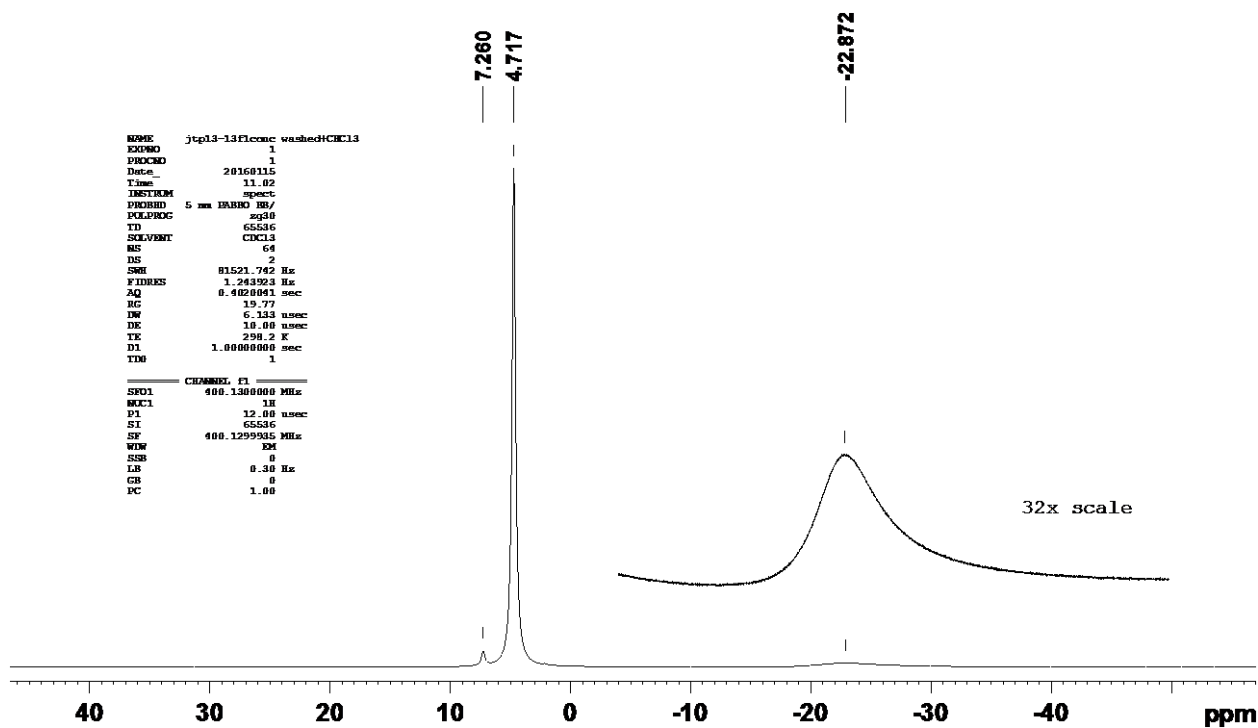


Figure S16. ¹H NMR spectrum (400 MHz, CDCl₃, ca. 0.9 M) of nitroxide 1 with one drop of CHCl₃ (label: JTP13-13f1).

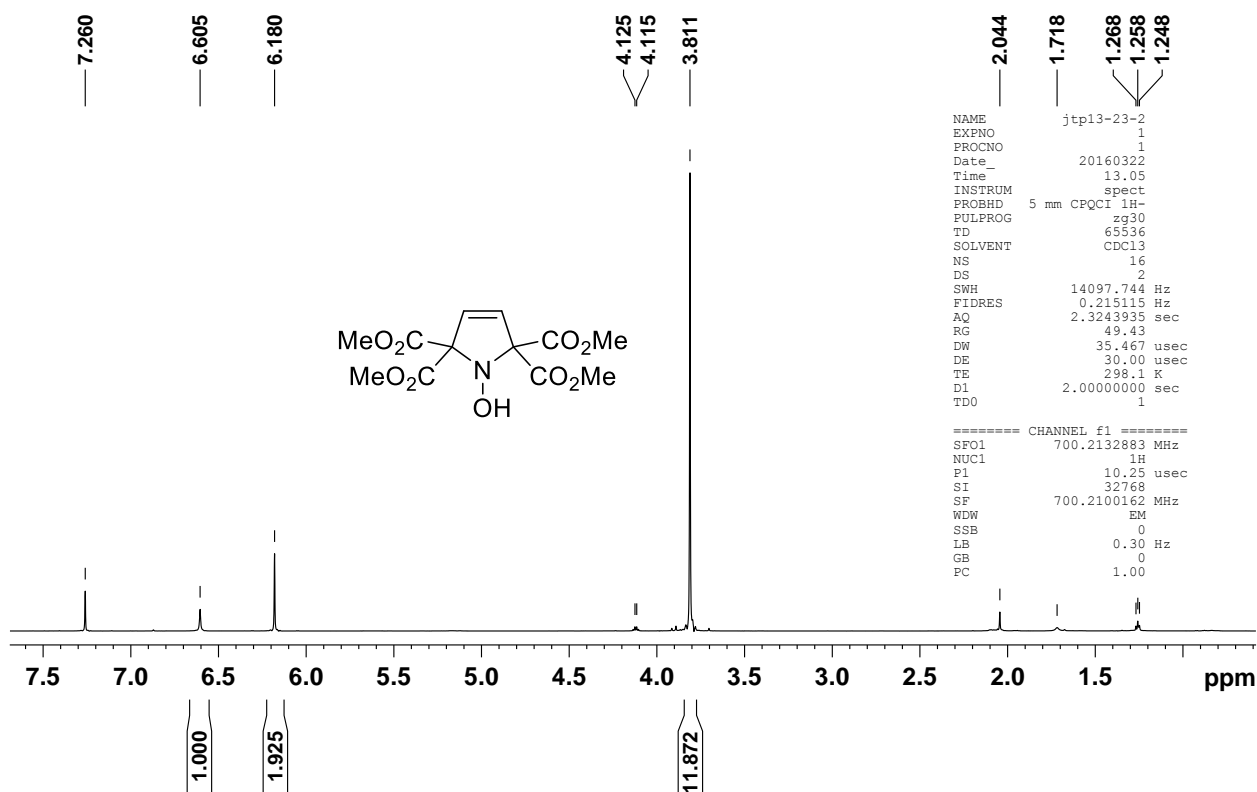


Figure S17. ¹H NMR spectrum (700 MHz, CDCl₃) of hydroxylamine **1-H** (label: JTP13-23-2).

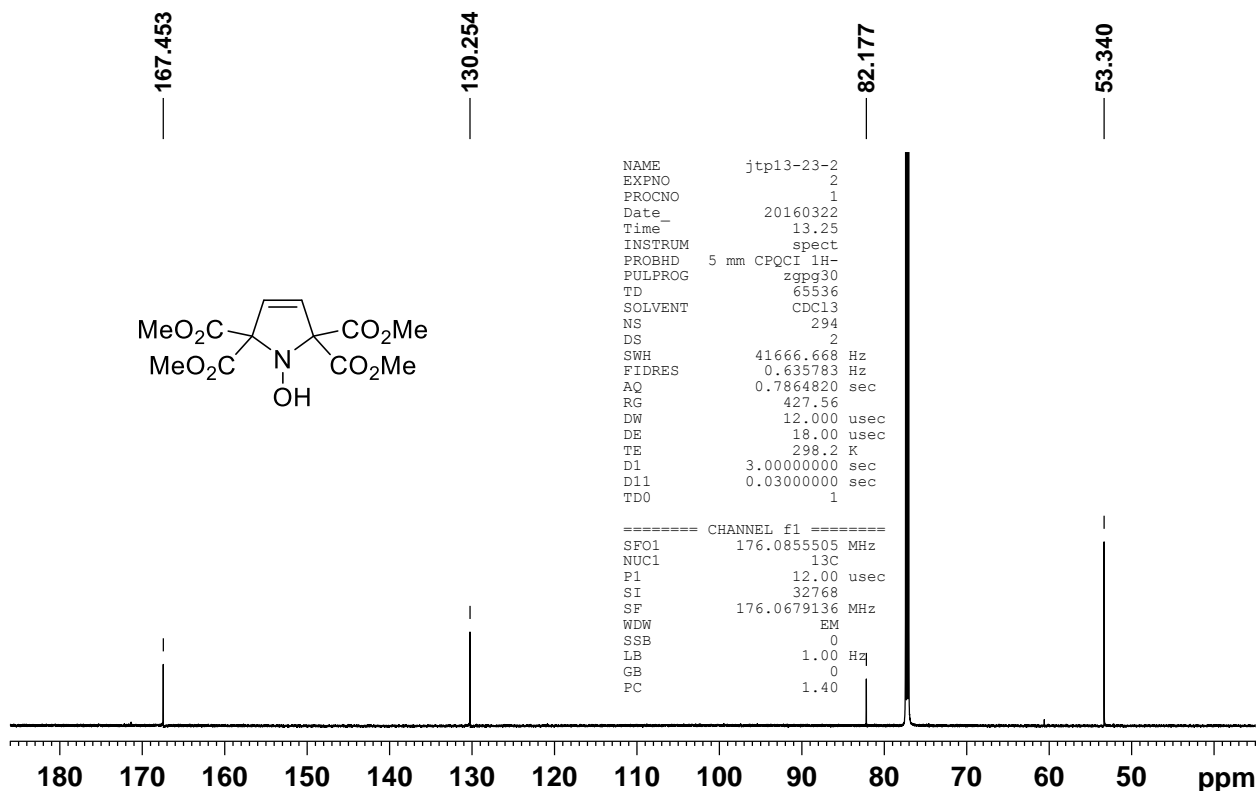


Figure S18. ¹³C NMR spectrum (176 MHz, CDCl₃) of hydroxylamine **1-H** (label: JTP13-23-2).

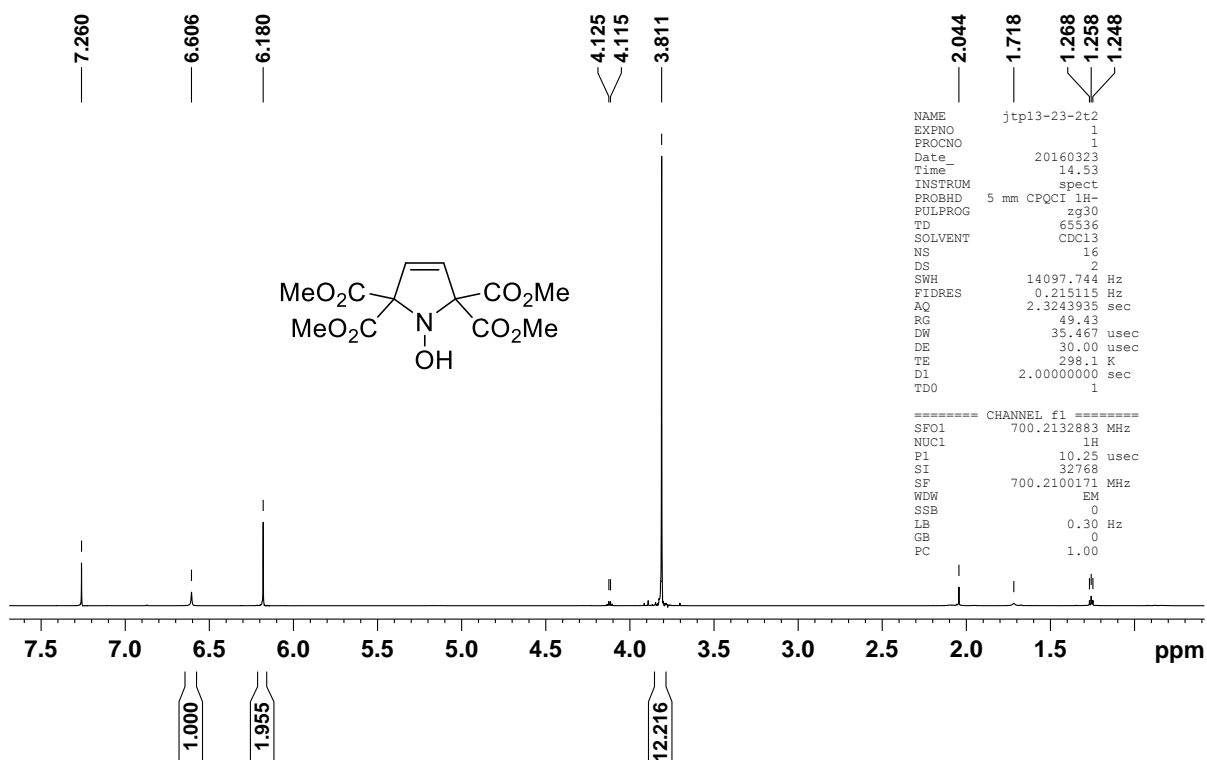


Figure S19. ^1H NMR spectrum (700 MHz, CDCl_3) of hydroxylamine **1-H** after overnight in freezer (label: JTP13-23-2).

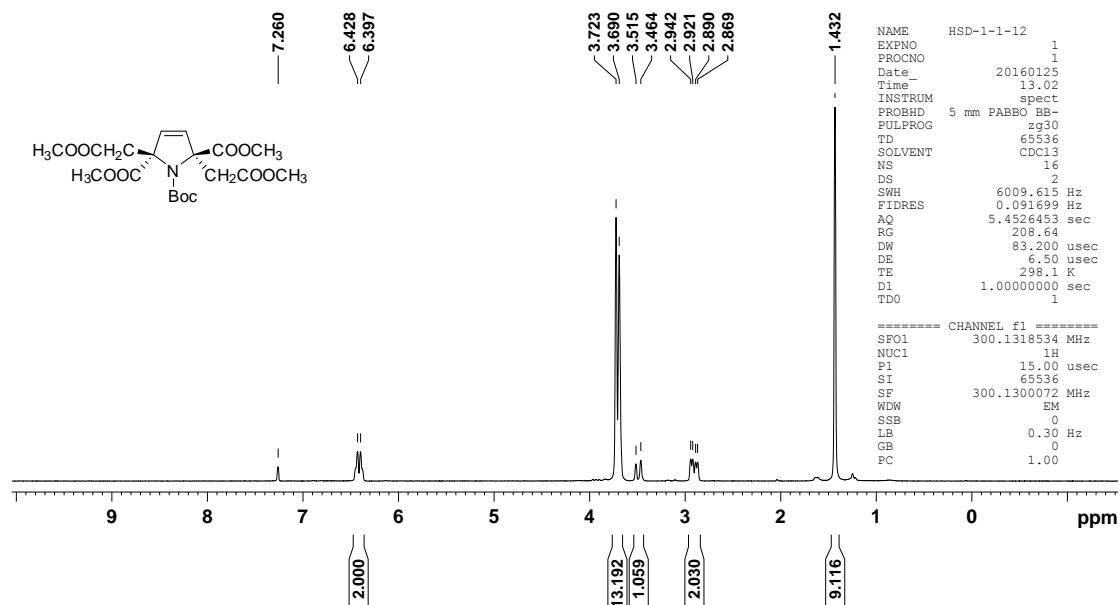


Figure S20. ^1H -NMR spectrum (300 MHz, CDCl_3) of compound **6** (Label: HSD-1-1-12).

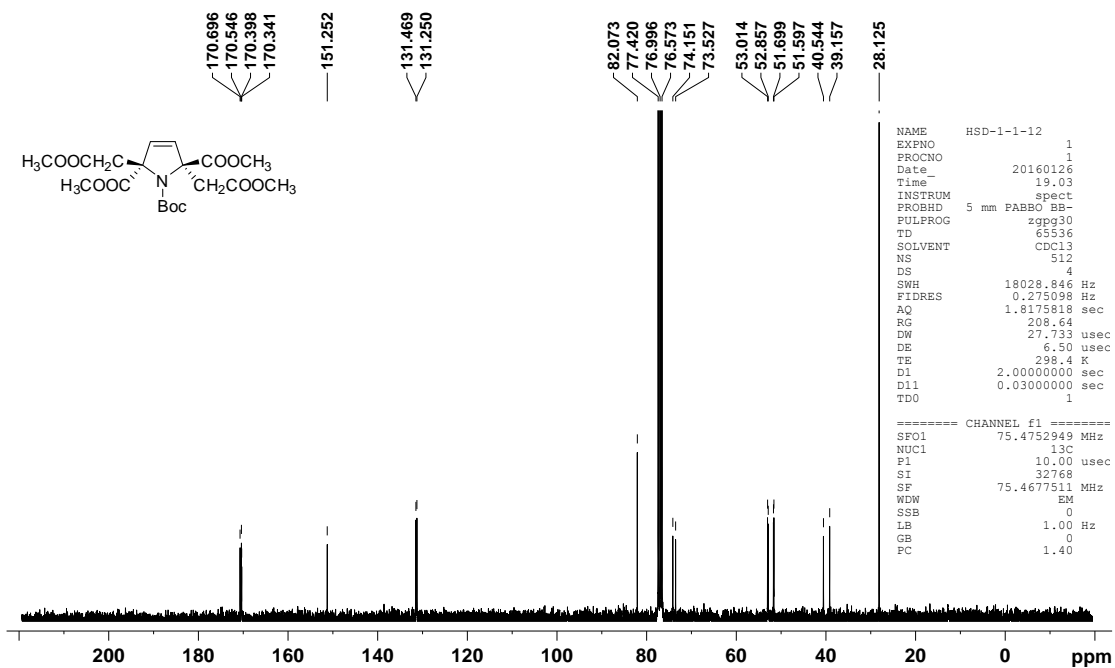


Figure S21. ¹³C-NMR spectrum (75 MHz, CDCl₃) of compound 6 (Label: HSD-1-1-12).

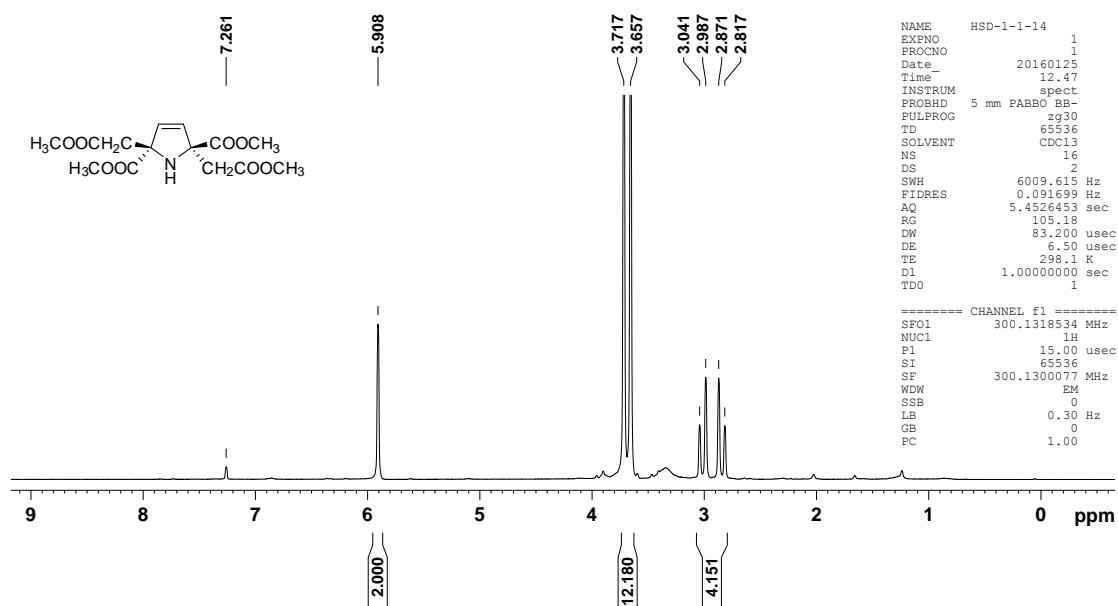


Figure S22. ¹H-NMR spectrum (300 MHz, CDCl₃) of compound 7 (Label: HSD-1-1-14).

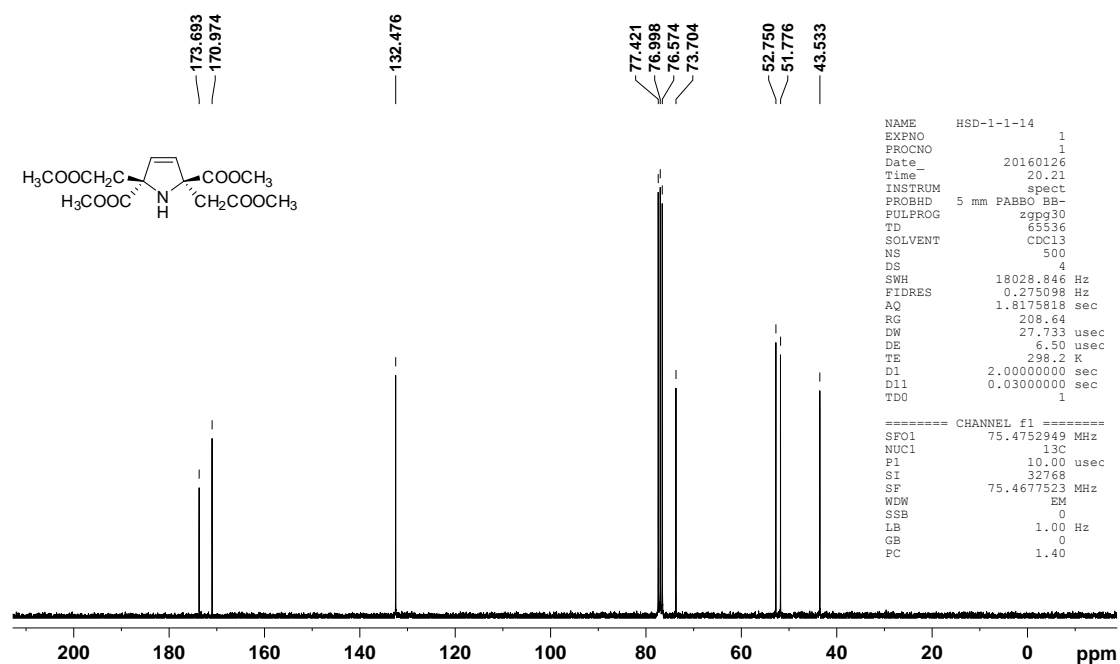


Figure S23. ^{13}C -NMR spectrum (75 MHz, CDCl_3) of compound 7 (Label: HSD-1-1-14).

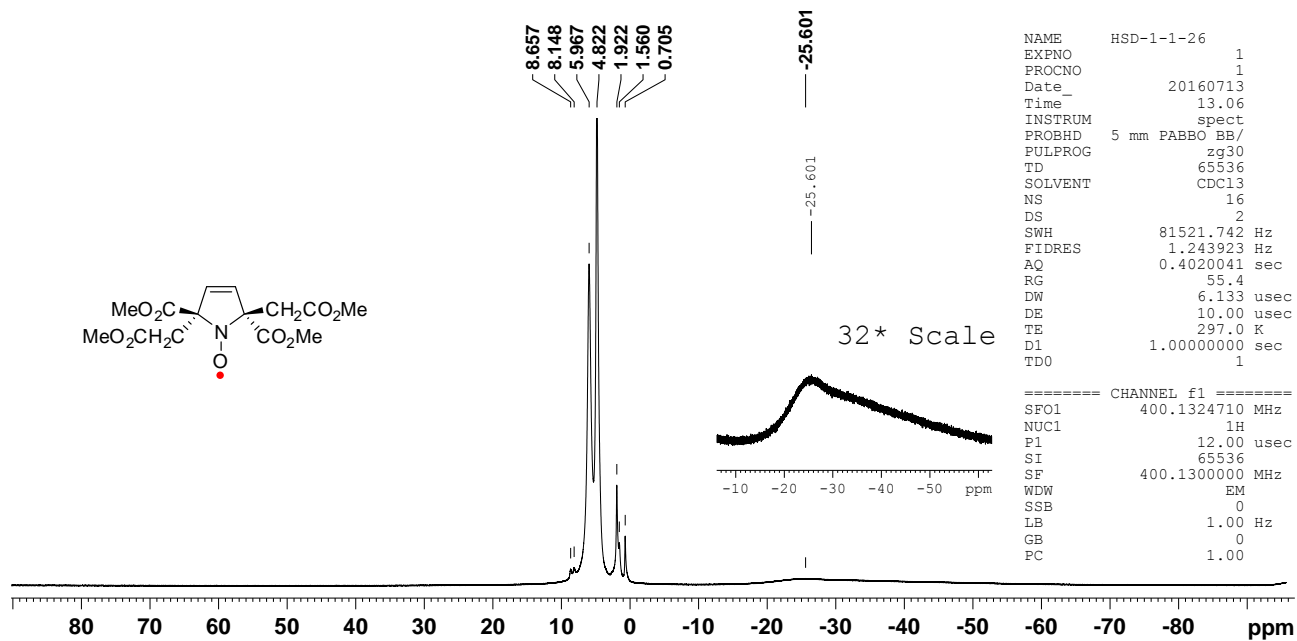


Figure S24. ^1H NMR spectrum (400 MHz, CDCl_3 , ca. 0.9 M) of nitroxide 2 (label: JTP13-13f1).

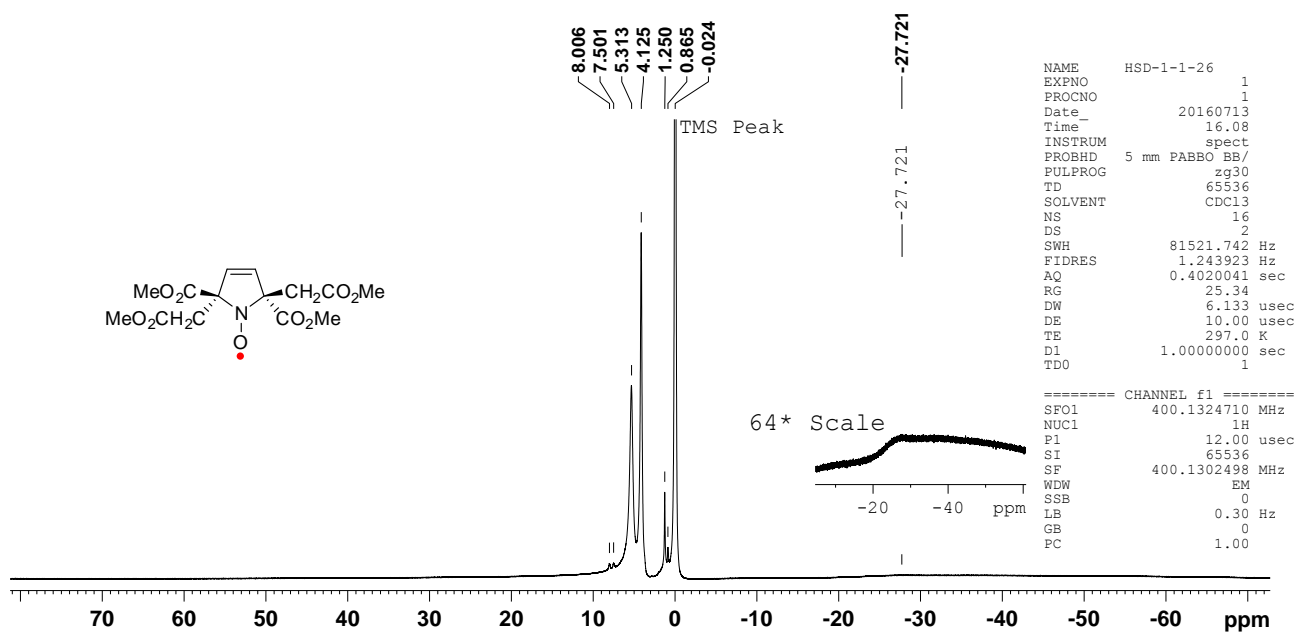


Figure S25. ^1H NMR spectrum (400 MHz, CDCl_3 , ca. 0.9 M) of nitroxide **2** with one drop of TMS (label: JTP13-13f1).

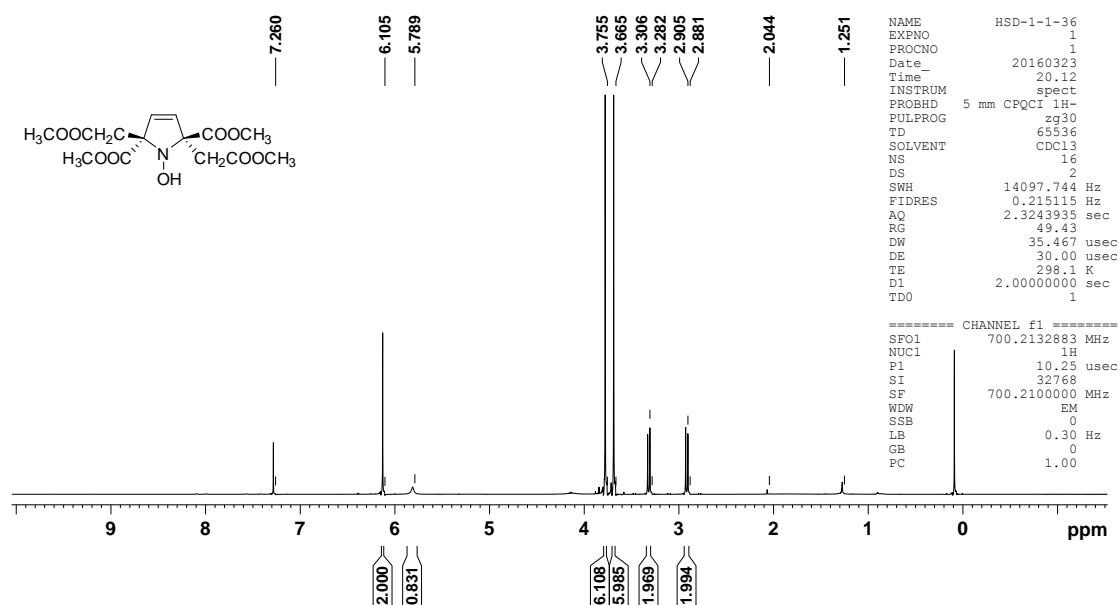


Figure S26. ^1H -NMR spectrum (700 MHz, CDCl_3) of compound **2-H** (Label: HSD-1-1-36).

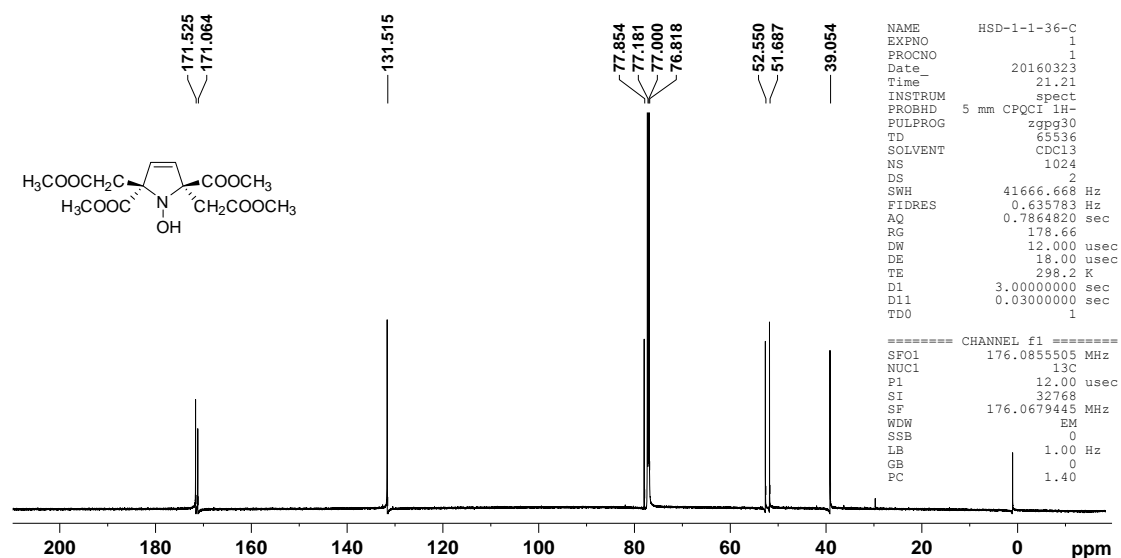


Figure S27. ^{13}C -NMR spectrum (176 MHz, CDCl_3) of compound **2-H** (Label: HSD-1-1-36).

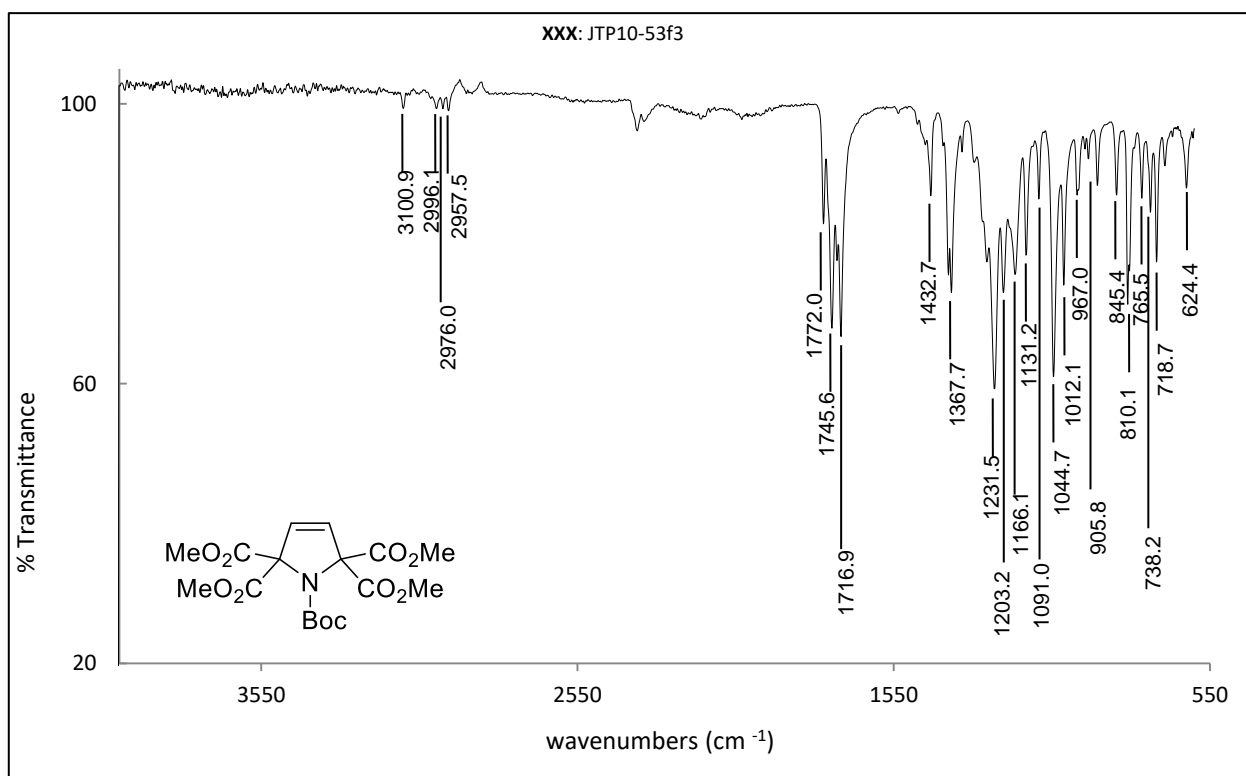


Figure S28. IR spectrum (ATR, diamond) of **4** (label: JTP10-53f3).

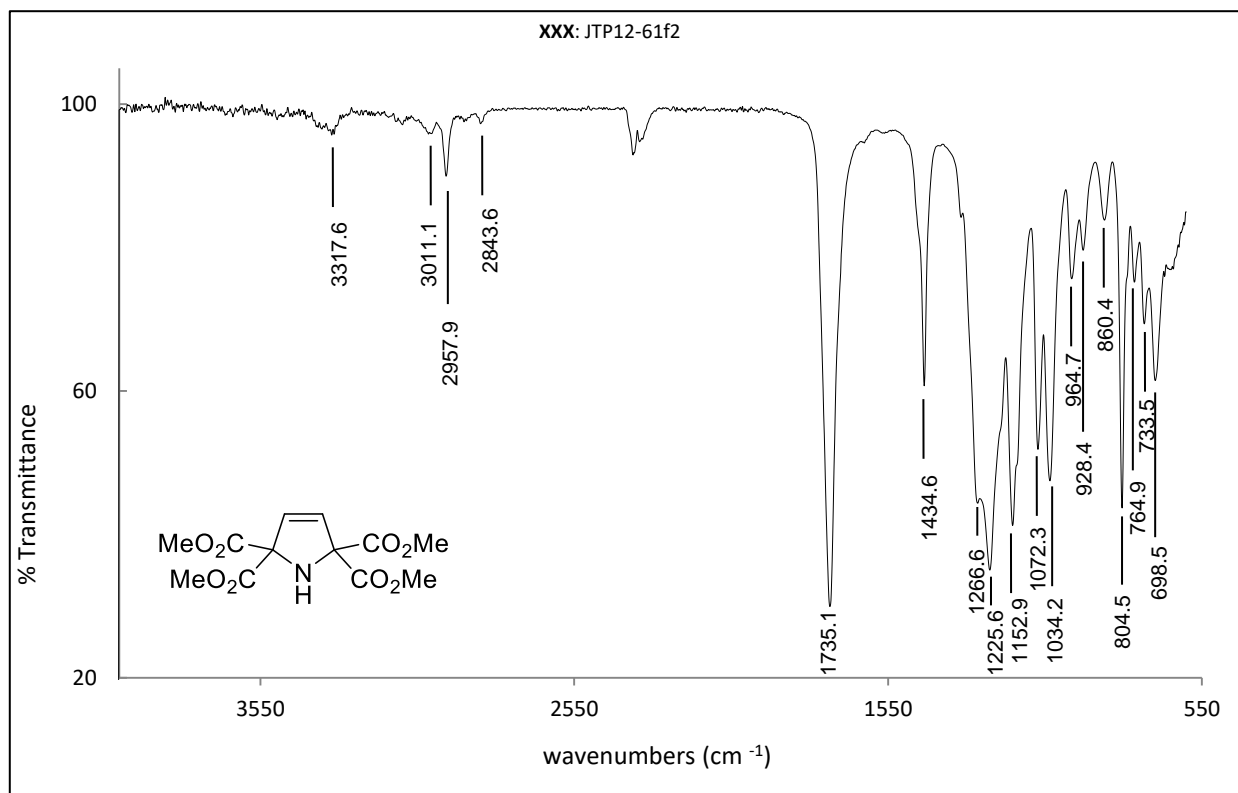


Figure S29. IR spectrum (ATR, diamond) of **5** (label: JTP12-61f2)

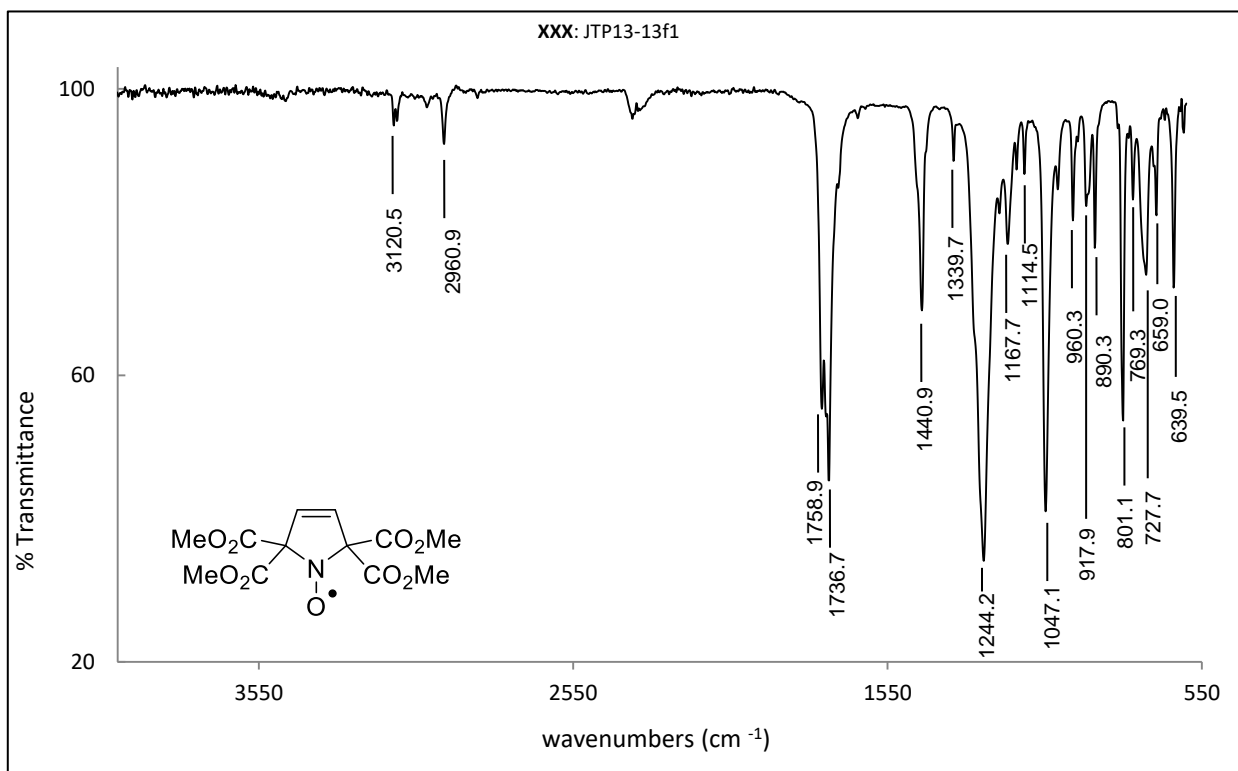


Figure S30. IR spectrum (ATR, diamond) of nitroxide **1** (label: JTP13-13f1)

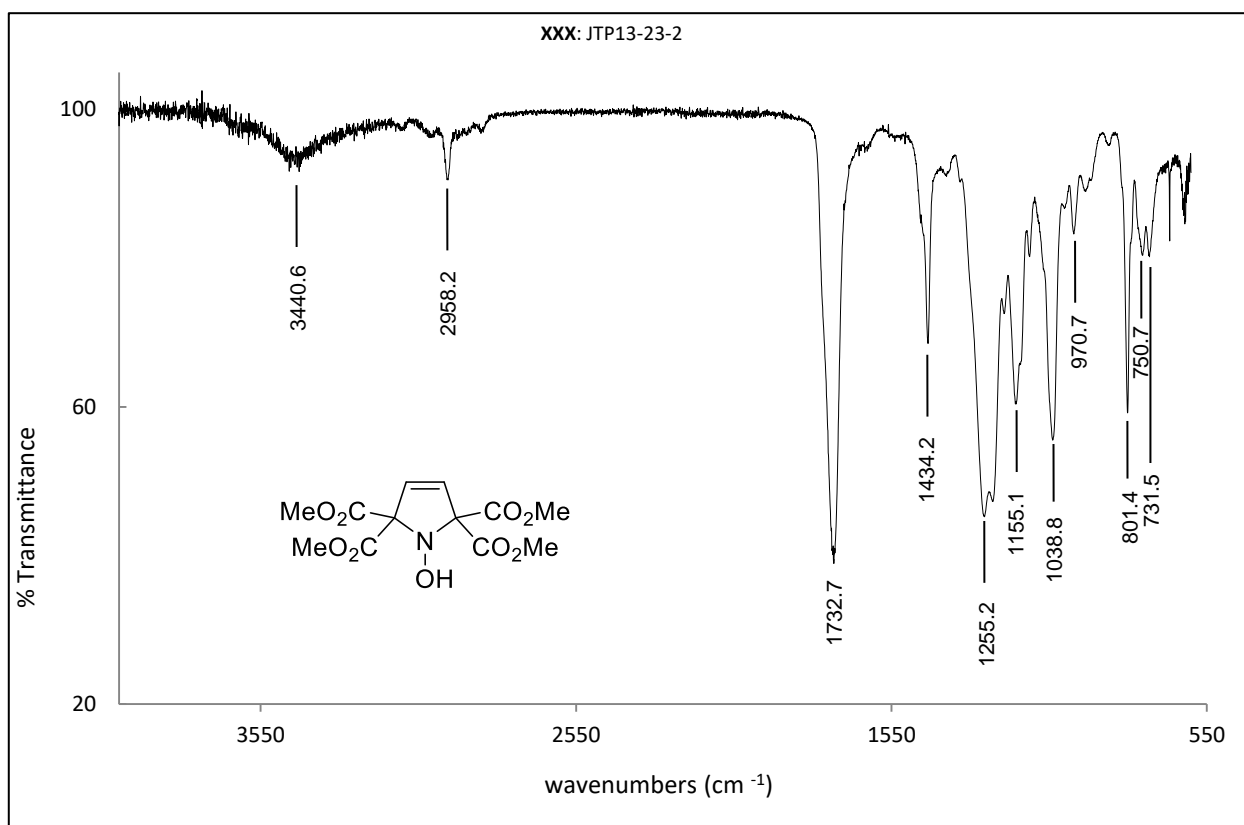
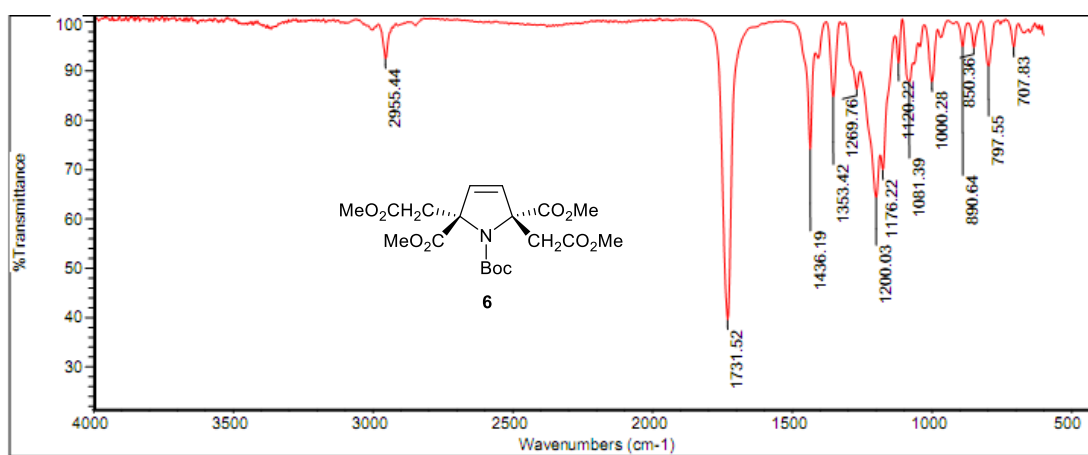


Figure S31. IR spectrum (ATR, diamond) of hydroxylamine **1-H** (label: JTP13-23-2).



Collection time: Tue Mar 22 20:45:35 2016 (GMT-05)

Mon Jul 18 19:34:01 2016 (GMT-05:00)

FIND PEAKS:

Spectrum: *HSD-1-1-12

Region: 4000.00 400.00

Absolute threshold: 96.697

Sensitivity: 50

Peak list:

Position	Intensity
707.83	94.895
797.55	91.017
850.36	94.706
890.64	94.852
1000.28	87.788
1081.39	87.887
1120.22	91.517
1176.22	69.972
1200.03	64.298
1269.76	85.310
1353.42	84.713
1436.19	74.004
1731.52	39.490
2955.44	92.483

Figure 32. IR spectrum (ATR, ZnSe) of compound **6** (label: HSD-1-1-12).

Multiple Mass Analysis: 3 mass(es) processed

Tolerance = 15.0 PPM / DBE: min = -1.5, max = 25.0

Element prediction: Off

Number of isotope peaks used for i-FIT = 3

Monoisotopic Mass, Even Electron Ions

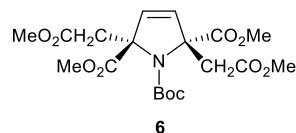
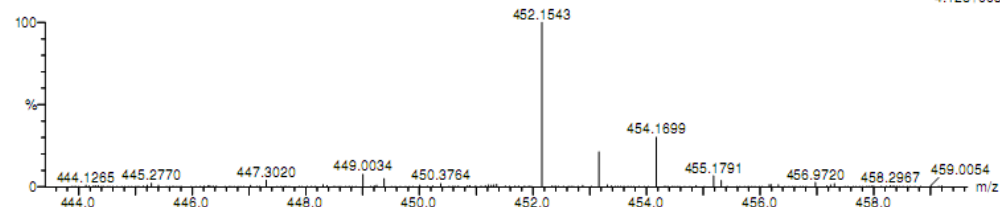
218018 formula(e) evaluated with 10 results within limits (all results (up to 1000) for each mass)

Elements Used:

12C: 0-40 13C: 0-1 1H: 0-60 14N: 0-1 16O: 0-11 23Na: 1-1

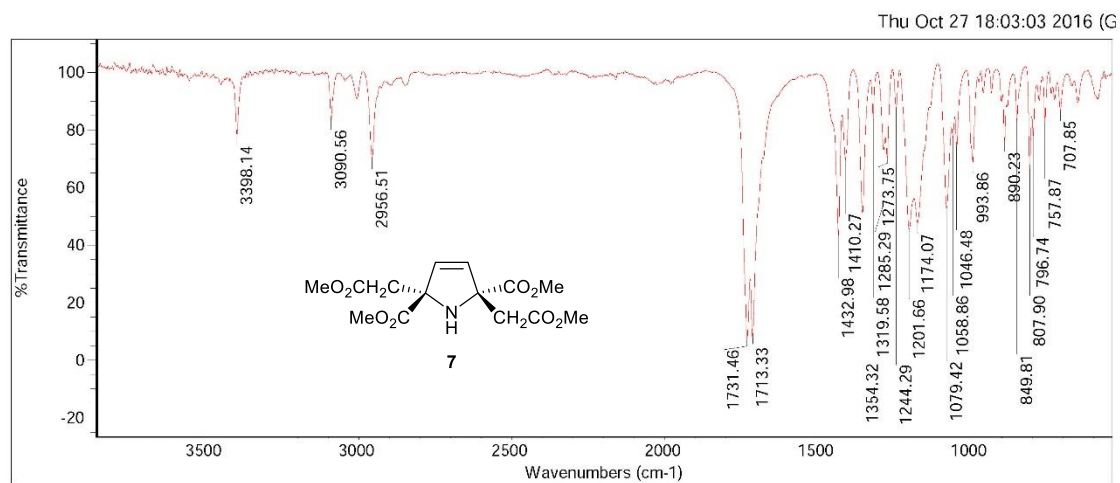
Huang / Rajca. HSD-1-1-12 ESI in Naacetate solution23-Feb-2016

60311 100 (1.913) AM (Cen,3, 60.00, Ht,5000.0,0.00,1.00); Sm (SG, 1x3.00); Cm (100:126)

6.00000000
TOF MS ES+
4.12e-003

Mass	RA	Calc. Mass	mDa	PPM	DBE	i-FIT	Formula
452.1543	100.00	452.1533	1.0	2.2	6.5	0.1	12C19 1H27 14N 16O10 23Na
		452.1555	-1.2	-2.7	15.5	0.1	12C26 13C 1H24 16O5 23Na
		452.1496	4.7	10.4	24.5	1.2	12C33 13C 1H20 23Na
453.1613	21.21	453.1619	-0.6	-1.3	23.5	0.0	12C34 1H22 23Na
		453.1566	4.7	10.4	6.5	0.3	12C18 13C 1H27 14N 16O10
		453.1660	-4.7	-10.4	19.5	0.3	23Na 12C29 13C 1H23 14N 16O2
		453.1678	-6.5	-14.3	14.5	0.5	23Na 12C27 1H26 16O5 23Na
454.1699	30.11	454.1689	1.0	2.2	5.5	0.0	12C19 1H29 14N 16O10 23Na
		454.1711	-1.2	-2.6	14.5	0.0	12C26 13C 1H26 16O5 23Na
		454.1653	4.6	10.1	23.5	0.3	12C33 13C 1H22 23Na

Figure S33. HRMS-ESI (1% CH₃COONa in 3:1 (v/v) MeOH/H₂O) of compound **6** (Label: HSD-1-1-12).



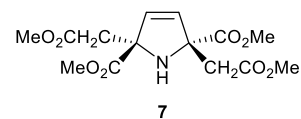
Collection time: Thu Oct 27 17:59:46 2016 (GMT-05)

Thu Oct 27 18:01:44 2016 (GMT-05:00)
FIND PEAKS:
Spectrum: *1ISD-1-1-14-IR spectrum1
Region: 4000.00 400.00
Absolute threshold: 80.733
Sensitivity: 50
Peak list:
Position: 707.85 Intensity: 88.598
Position: 757.87 Intensity: 82.209
Position: 796.74 Intensity: 77.551
Position: 807.90 Intensity: 65.734
Position: 849.81 Intensity: 82.061
Position: 890.23 Intensity: 75.202
Position: 993.86 Intensity: 60.504
Position: 1046.48 Intensity: 74.052
Position: 1058.86 Intensity: 76.990
Position: 1079.42 Intensity: 52.496
Position: 1174.07 Intensity: 47.447
Position: 1201.66 Intensity: 45.270
Position: 1244.29 Intensity: 87.825
Position: 1273.75 Intensity: 70.086
Position: 1285.29 Intensity: 77.885
Position: 1319.58 Intensity: 65.888
Position: 1354.32 Intensity: 50.582
Position: 1410.27 Intensity: 65.313
Position: 1432.98 Intensity: 43.122
Position: 1713.33 Intensity: 7.348
Position: 1731.46 Intensity: 6.819
Position: 2956.51 Intensity: 70.074
Position: 3090.56 Intensity: 83.171
Position: 3398.14 Intensity: 77.935

Figure S34. IR spectrum (ATR, ZnSe) of compound **7** (Label: HSD-1-1-14).

Elemental Composition Report

Multiple Mass Analysis: 2 mass(es) processed
 Tolerance = 50.0 PPM / DBE: min = -1.5, max = 50.0
 Isotope cluster parameters: Separation = 1.0 Abundance = 1.0%



Monoisotopic Mass, Odd and Even Electron Ions
 137 formula(e) evaluated with 15 results within limits (all results (up to 1000) for each mass)

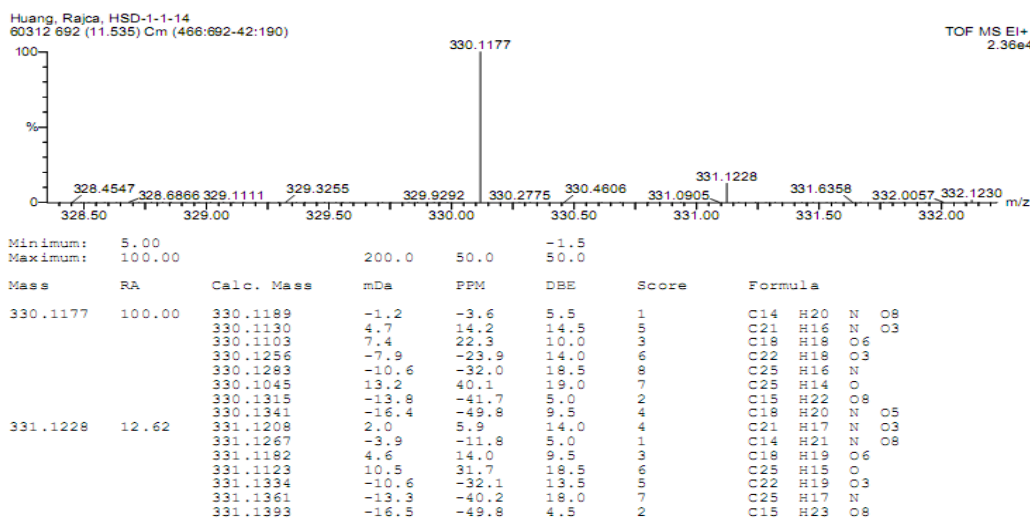


Figure S35. HRMS-EI (1% CH₃COONa in 3:1 (v/v) MeOH/H₂O) of compound 7 (Label: HSD-1-14).

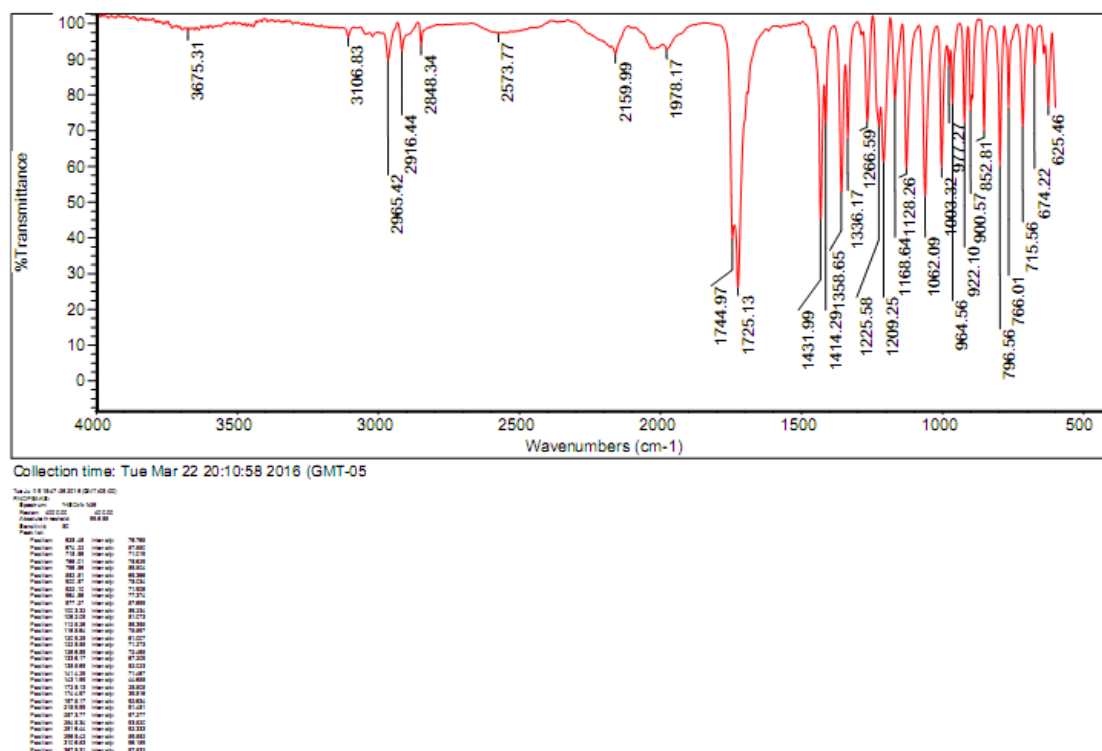


Figure S36. IR spectrum (ATR, ZnSe) of nitroxide 2 (label: HSD-1-26).

Multiple Mass Analysis: 3 mass(es) processed

Tolerance = 15.0 PPM / DBE: min = -1.5, max = 25.0

Element prediction: Off

Number of isotope peaks used for i-FIT = 3

Monoisotopic Mass, Odd and Even Electron Ions

156193 formula(e) evaluated with 13 results within limits (all results (up to 1000) for each mass)

Elements Used:

12C: 0-40 13C: 0-1 1H: 0-60 14N: 0-1 16O: 0-11 23Na: 1-1

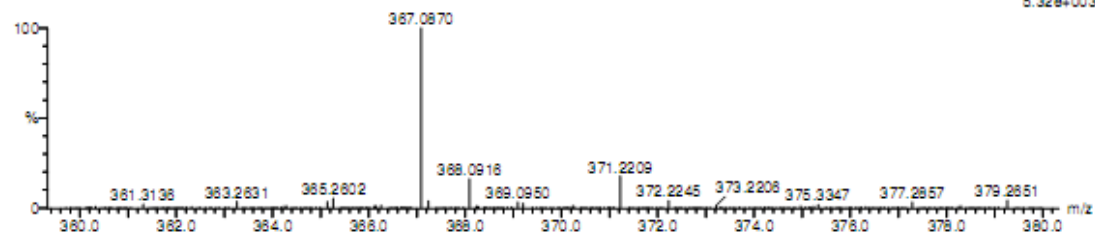
Huang / Rajca HSD-1-1-15 ESI in Naacetate solution 23-Feb-2016

60313 28 (0.502) AM (Can, 3, 60.00, HI, 5000.0, 0.00, 1.00); Sm (SG, 1x3.00); Cm (10:27)

8.00000000

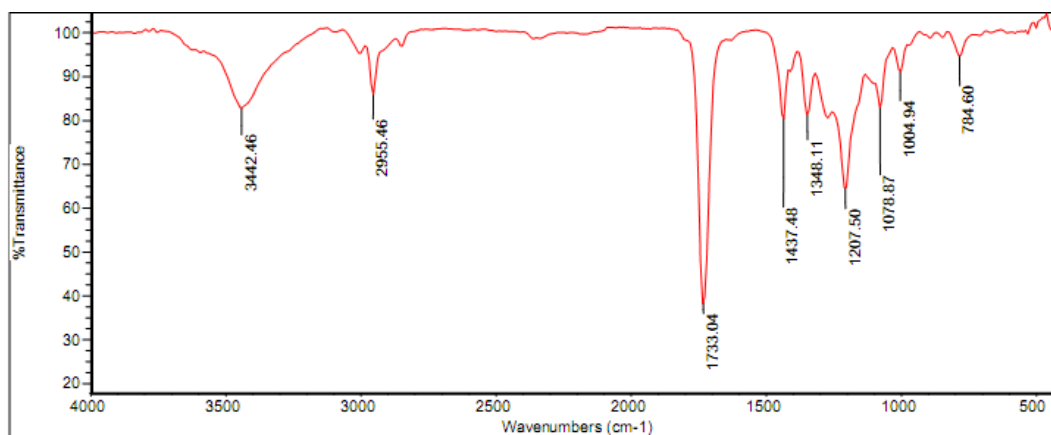
TOF MS ES+

5.32e+003



Mass	RA	Calc. Mass	mDa	PPM	DBE	i-FIT	Formula
367.0870	100.00	367.0879	-0.9	-2.3	6.0	0.1	12C14 1H18 14N 16O9 23Na
		367.0902	-3.2	-8.7	15.0	1.0	12C21 13C 1H15 16O4 23Na
		367.0835	3.5	9.5	6.5	1.3	12C13 13C 1H17 14N 16O9 23Na
368.0916	16.10	367.0821	4.9	13.3	15.0	2.6	12C21 1H14 14N 16O4 23Na
		368.0913	0.3	0.8	6.0	0.0	12C13 13C 1H18 14N 16O9 23Na
		368.0899	1.7	4.6	14.5	0.1	12C21 1H15 14N 16O4 23Na
		368.0958	-4.2	-11.4	5.5	0.3	12C14 1H19 14N 16O9 23Na
		368.0872	4.4	12.0	10.0	0.3	12C18 1H17 16O7 23Na
371.2209	17.65	371.2198	1.1	3.0	5.5	0.0	12C21 1H32 16O4 23Na
		371.2225	-1.6	-4.3	10.0	0.0	12C24 1H30 14N 16O 23Na
		371.2180	2.9	7.8	10.5	0.2	12C23 13C 1H29 14N 16O 23Na
		371.2239	-3.0	-8.1	1.5	0.2	12C16 13C 1H33 14N 16O6 23Na
		371.2154	5.5	14.8	6.0	0.6	12C20 13C 1H31 16O4 23Na

Figure S37. HRMS-ESI (1% CH₃COONa in 3:1 (v/v) MeOH/H₂O) of nitroxide **2** (Label: HSD-1-1-15).



Collection time: Mon Jul 18 18:52:41 2016 (GMT-05:00)

Mon Jul 18 19:53:36 2016 (GMT-05:00)

RIND PEAKS:

Spectrum: **HSD-1-1-36

Region: 4000.00 400.00

Absolute threshold: -0.002

Sensitivity: 50

Peak list:

Position	Intensity
784.60	0.0241
1004.94	0.0413
1078.87	0.0819
1207.50	0.193
1348.11	0.0908
1437.48	0.0980
1733.04	0.425
2955.46	0.0866
3442.46	0.0820

Figure S38. IR spectrum (ATR, ZnSe) of compound **2-H** (label: HSD-1-1-36).

Multiple Mass Analysis: 3 mass(es) processed
 Tolerance = 50.0 PPM / DBE: min = -1.5, max = 50.0
 Isotope cluster parameters: Separation = 1.0 Abundance = 1.0%

Monoisotopic Mass, Odd and Even Electron Ions
 259 formula(e) evaluated with 20 results within limits (all results (up to 1000) for each mass)

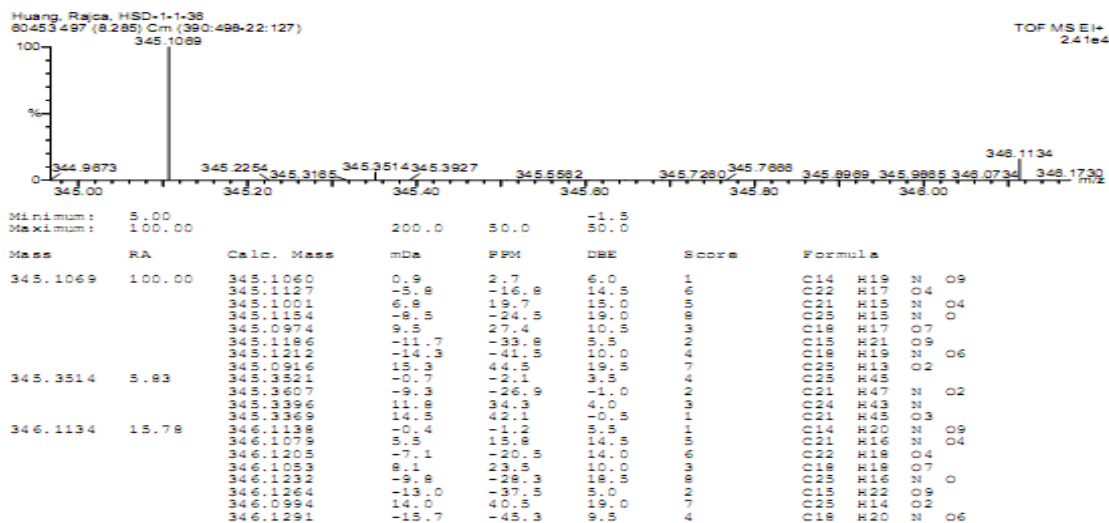


Figure S39. HRMS-EI (1% CH₃COONa in 3:1 (v/v) MeOH/H₂O) of compound 2-H (Label: HSD-1-1-36).

9. Supporting References.

- S1. SAINT, Bruker Analytical X-Ray Systems, Madison, WI, current version.
- S2. SADABS, Bruker Analytical X-Ray Systems, Madison, WI, current version; empirical correction for absorption anisotropy: Blessing, R. *Acta Cryst.* **1995**, *A51*, 33–38.
- S3. *SHELX*: Sheldrick, G. M. *Acta Cryst.* **2008**, *A64*, 112–122.
- S4. <http://chemmatcars.uchicago.edu/>
- S5. <http://www.iumsc.indiana.edu/projects/SCrAPS/index.html>
- S6. Toy, A. D., Chaston, S. H. H., Pilbrow, J. R., Smith, T.D. Electron spin resonance study of the copper(II) chelates of certain monothio- β -diketones and diethyldithiocarbamate. *Inorg. Chem.* **1971**, *10*, 2219-2225.
- S7. Frisch, M. J., et al. *Gaussian 09*, Revision A.01; Gaussian, Inc.: Wallingford, CT, 2009.
- S8. (a) Donohoe, T. J.; Headley, C. E.; Cousins, R. P. C.; Cowley, A. Flexibility in the Partial Reduction of 2,5-Disubstituted Pyrroles: Application to the Synthesis of DMDP. *Org. Lett.* **2003**, *5*, 999–1002. (b) Donohoe, T. J.; Thomas, R. E.; Cheeseman, M. D.; Rigby, C. L.; Bhalay, G.; Linney, I. D. Flexible Strategy for the Synthesis of Pyrrolizidine Alkaloids. *Org. Lett.* **2008**, *10*, 3615–3618.
- S9. Rajca, A.; Shiraishi, K.; Rajca, S. Stable Diarylnitroxide Diradical with Triplet Ground State. *Chem. Commun.* **2009**, 4372–4374.

10. Cartesian Coordinates for UB3LYP/6-311G(d,p)+ZPVE Geometries of the Lowest Energy Conformations of Nitroxides 1 and 2.

Nitroxide 1 C₂, Of11 (Table S4):

```

Stoichiometry C12H14NO9(2)
Framework group C2[C2(NO),X(C12H14O8)]
Deg. of freedom 51
Full point group C2 NOp 2
Largest Abelian subgroup C2 NOp 2
Largest concise Abelian subgroup C2 NOp 2
Standard orientation:
-----
Center Atomic Atomic Coordinates (Angstroms)
Number Number Type X Y Z
-----
1 6 0 0.030375 1.230842 -0.508620
2 6 0 0.000000 0.663404 -1.904304
3 6 0 0.000000 -0.663404 -1.904304
4 6 0 -0.030375 -1.230842 -0.508620
5 1 0 -0.001355 1.310298 -2.769273
6 1 0 0.001355 -1.310298 -2.769273
7 7 0 0.000000 0.000000 0.315272
8 8 0 0.000000 0.000000 1.576706
9 6 0 -1.218428 2.091651 -0.206675
10 6 0 1.307612 2.077690 -0.332340
11 6 0 -1.307612 -2.077690 -0.332340
12 6 0 1.218428 -2.091651 -0.206675
13 8 0 1.405236 3.178877 -0.809369
14 8 0 -2.199849 2.112563 -0.900589
15 8 0 -1.405236 -3.178877 -0.809369
16 8 0 2.199849 -2.112563 -0.900589
17 8 0 2.268467 1.425864 0.317510
18 8 0 -1.064299 2.761591 0.935748
19 8 0 -2.268467 -1.425864 0.317510
20 8 0 1.064299 -2.761591 0.935748
21 6 0 3.519903 2.130805 0.454641
22 6 0 -2.187728 3.561985 1.353552
23 6 0 -3.519903 -2.130805 0.454641
24 6 0 2.187728 -3.561985 1.353552
25 1 0 3.063918 -2.930520 1.504454
26 1 0 3.933017 2.359197 -0.528370
27 1 0 -3.063918 2.930520 1.504454
28 1 0 -3.933017 -2.359197 -0.528370
29 1 0 4.171708 1.453864 1.000449
30 1 0 -4.171708 -1.453864 1.000449
31 1 0 -2.410310 4.319182 0.600949
32 1 0 2.410310 -4.319182 0.600949
33 1 0 1.880121 -4.023952 2.288078
34 1 0 -3.369656 -3.057295 1.009510
35 1 0 -1.880121 4.023952 2.288078
36 1 0 3.369656 3.057295 1.009510
-----
Rotational constants (GHZ): 0.3783914 0.2702090 0.1940770
Standard basis: 6-311G(d,p) (5D, 7F)

SCF Done: E(UB3LYP) = -1197.70468172 A.U. after 4 cycles
Convg = 0.3256D-08 -V/T = 2.0032
<Sx>= 0.0000 <Sy>= 0.0000 <Sz>= 0.5000 <S**2>= 0.7537 S= 0.5019
<L.S>= 0.000000000000E+00
Annihilation of the first spin contaminant:
S**2 before annihilation 0.7537, after 0.7500
Item Value Threshold Converged?
Maximum Force 0.000000 0.000015 YES
RMS Force 0.000000 0.000010 YES
Maximum Displacement 0.000058 0.000060 YES
RMS Displacement 0.000013 0.000040 YES
Predicted change in Energy=-7.710011D-12
Optimization completed.
-- Stationary point found.

```

Nitroxide 2 C₂, Rot8 (Table S5): geometry optimization starting from X-ray structure geometry

```

Stoichiometry C14H18NO9(2)
Framework group C2[C2(NO),X(C14H18O8)]
Deg. of freedom 60
Full point group C2 NOp 2
Largest Abelian subgroup C2 NOp 2
Largest concise Abelian subgroup C2 NOp 2
Standard orientation:
-----
Center Atomic Atomic Coordinates (Angstroms)
Number Number Type X Y Z
-----
 1 6 0 0.000000 1.243858 0.019612
 2 6 0 0.012295 0.664381 -1.373934
 3 6 0 -0.012295 -0.664381 -1.373934
 4 6 0 0.000000 -1.243858 0.019612
 5 1 0 0.017185 1.310765 -2.238503
 6 1 0 -0.017185 -1.310765 -2.238503
 7 7 0 0.000000 0.000000 0.832110
 8 8 0 0.000000 0.000000 2.098336
 9 6 0 -1.240824 2.081815 0.367091
10 6 0 1.276273 2.049984 0.363580
11 6 0 -1.276273 -2.049984 0.363580
12 6 0 1.240824 -2.081815 0.367091
13 8 0 1.273538 3.152807 0.842562
14 8 0 -1.273538 -3.152807 0.842562
15 8 0 2.385082 1.351183 0.078685
16 8 0 -2.385082 -1.351183 0.078685
17 6 0 3.631499 1.998840 0.405950
18 1 0 4.409089 1.310564 0.083794
19 1 0 3.712975 2.949404 -0.121903
20 1 0 3.692788 2.175800 1.480412
21 6 0 -3.631499 -1.998840 0.405950
22 1 0 -4.409089 -1.310564 0.083794
23 1 0 -3.712975 -2.949404 -0.121903
24 1 0 -3.692788 -2.175800 1.480412
25 1 0 -2.128205 1.473670 0.170010
26 1 0 -1.231442 2.319062 1.430517
27 1 0 1.231442 -2.319062 1.430517
28 1 0 2.128205 -1.473670 0.170010
29 6 0 1.353353 -3.358058 -0.438950
30 6 0 -1.353353 3.358058 -0.438950
31 8 0 -0.852089 3.556945 -1.519383
32 8 0 0.852089 -3.556945 -1.519383
33 8 0 -2.139538 4.247467 0.191348
34 8 0 2.139538 -4.247467 0.191348
35 6 0 -2.341957 5.497783 -0.494056
36 1 0 -3.003043 6.075763 0.147447
37 1 0 -1.389902 6.012602 -0.629017
38 1 0 -2.799995 5.330199 -1.469941
39 6 0 2.341957 -5.497783 -0.494056
40 1 0 3.003043 -6.075763 0.147447
41 1 0 1.389902 -6.012602 -0.629017
42 1 0 2.799995 -5.330199 -1.469941
-----
Rotational constants (GHZ): 0.3940737 0.1519222 0.1240881
Standard basis: 6-311G(d,p) (5D, 7F)
SCF Done: E(UB3LYP) = -1276.37925199 A.U. after 5 cycles
Convq = 0.3239D-08 -V/T = 2.0033
<Sx>= 0.0000 <Sy>= 0.0000 <Sz>= 0.5000 <S**2>= 0.7541 S= 0.5020
<L.S>= 0.000000000000E+00
Annihilation of the first spin contaminant:
S**2 before annihilation 0.7541, after 0.7500
Item Value Threshold Converged?
Maximum Force 0.000001 0.000015 YES
RMS Force 0.000000 0.000010 YES
Maximum Displacement 0.000047 0.000060 YES
RMS Displacement 0.000010 0.000040 YES
Predicted change in Energy=-4.753880D-11
Optimization completed.
-- Stationary point found.

```